

Host- and virus-induced gene silencing of HOG1-MAPK cascade genes in *Rhizophagus irregularis* inhibit arbuscule development and reduce resistance of plants to drought stress

Sijia Wang[†] , Xianan Xie[†], Xianrong Che, Wenzhen Lai, Ying Ren, Xiaoning Fan, Wentao Hu, Ming Tang*  and Hui Chen* 

State Key Laboratory of Conservation and Utilization of Subtropical Agro-Bioresources, Guangdong Laboratory for Lingnan Modern Agriculture, Guangdong Key Laboratory for Innovative Development and Utilization of Forest Plant Germplasm, College of Forestry and Landscape Architecture, South China Agricultural University, Guangzhou, China

Received 27 February 2022;

revised 18 November 2022;

accepted 24 December 2022.

*Correspondence (Tel +86 13519116730;

Fax +86 020 85280256; email

chenhui@scau.edu.cn (H. C.); Tel +86

13709229152; Fax +86 020 85280256;

email tangming@scau.edu.cn (M. T.))

[†]These authors contributed equally to this work.

Summary

Arbuscular mycorrhizal (AM) fungi can form beneficial associations with the most terrestrial vascular plant species. AM fungi not only facilitate plant nutrient acquisition but also enhance plant tolerance to various environmental stresses such as drought stress. However, the molecular mechanisms by which AM fungal mitogen-activated protein kinase (MAPK) cascades mediate the host adaptation to drought stimulus remains to be investigated. Recently, many studies have shown that virus-induced gene silencing (VIGS) and host-induced gene silencing (HIGS) strategies are used for functional studies of AM fungi. Here, we identify the three HOG1 (High Osmolarity Glycerol 1)-MAPK cascade genes *RiSte11*, *RiPbs2* and *RiHog1* from *Rhizophagus irregularis*. The expression levels of the three HOG1-MAPK genes are significantly increased in mycorrhizal roots of the plant *Astragalus sinicus* under severe drought stress. RiHog1 protein was predominantly localized in the nucleus of yeast in response to 1 M sorbitol treatment, and RiPbs2 interacts with RiSte11 or RiHog1 directly by pull-down assay. Importantly, VIGS or HIGS of *RiSte11*, *RiPbs2* or *RiHog1* hampers arbuscule development and decreases relative water content in plants during AM symbiosis. Moreover, silencing of HOG1-MAPK cascade genes led to the decreased expression of drought-resistant genes (*RiAQPs*, *RiTSPs*, *RiNTH1* and *Ri14-3-3*) in the AM fungal symbiont in response to drought stress. Taken together, this study demonstrates that VIGS or HIGS of AM fungal HOG1-MAPK cascade inhibits arbuscule development and expression of AM fungal drought-resistant genes under drought stress.

Keywords: Arbuscular mycorrhizal fungi, *Rhizophagus irregularis*, HOG1-MAPK genes, virus-induced gene silencing, host-induced gene silencing, drought stress.

Introduction

In natural ecosystems, terrestrial vascular plants as sessile organisms are faced with highly variable environmental conditions, such as biotic and abiotic stresses (Zhu, 2016). Among the abiotic stresses, drought stress (DS) is harmful to plant growth and productivity. For example, drought inhibits photosynthesis, disrupts water balance and affects stomatal conductance, all of which lead to the decreased growth of plants (Chitarra *et al.*, 2016; Quiroga *et al.*, 2019). However, vascular plants have evolved many strategies to adapt to the DS. The establishment of arbuscular mycorrhizal (AM) symbiosis can improve plant nutrient uptake and other physiological alterations to cope with DS (Begum *et al.*, 2021; Püschel *et al.*, 2021).

Arbuscular mycorrhizal fungi are capable of forming beneficial associations with more than 72% of terrestrial vascular plants (Brundrett and Tedersoo, 2018; Genre *et al.*, 2020). The obligate biotrophic AM fungi need to consume sugars and lipids from host plants to complete their life cycles (An *et al.*, 2019; Bago *et al.*, 2003; Jiang *et al.*, 2017; Luginbuehl *et al.*, 2017), and in turn AM fungi facilitate plant growth and health not only by increasing mineral nutrient acquisition (particularly Pi) from surrounding soil but also protecting plants against multiple

abiotic stresses (Lenoir *et al.*, 2016; Wang *et al.*, 2017). Therefore, AM fungi are key endosymbionts of plant symbiosis and provide a friendly and sustainable way to agriculture development (Begum *et al.*, 2019; Gianinazzi *et al.*, 2010). AM symbiosis can improve the host plant's tolerance to drought by regulating plant physiological and molecular responses, such as the plant parameters: stomatal conductance, transpiration, photosynthesis, leaf or root hydration, root aquaporins (AQPs) and accentuating root uptake of mineral nutrients, in particular phosphate (Augé, 2001; Püschel *et al.*, 2021). Despite the great importance of AM symbiosis, the underlying molecular mechanisms by which AM fungi respond to DS remain poorly understood. However, arbuscular mycorrhizas have developed a common set of responsive mechanisms involved in resistance to DS to sense and relay this pressure signal, one of the most important signalling modules that transmit the perceived DS to the nucleus is the mitogen-activated protein kinase (MAPK) cascade (Liu *et al.*, 2015b).

Mitogen-activated protein kinase are serine/threonine protein kinases in all eukaryotes, which are evolutionarily conserved signalling hubs that regulate multiple stress responses in both plants and microorganisms (Lin *et al.*, 2021; Martínez-Soto and Ruiz-Herrera, 2017). MAPK cascades play critical roles in a series

of cellular signal transduction and cell growth regulation. A typical MAPK cascade reaction consists of three protein kinases: the MAPKKK-MAPKK-MAPK (Colcombet and Hirt, 2008). Among these MAPK cascades, the HOG (High Osmolarity Glycerol) pathway plays an important role in the plant responses to osmotic stress. In most filamentous fungi, HOG1-MAPK cascade is necessary for osmoregulation and hyphal growth or pathogenesis (Ji *et al.*, 2012; Jiang *et al.*, 2018; Zhou *et al.*, 2019). In *Saccharomyces cerevisiae*, the Hog1 pathway is regulated by three MAPKKs (Ste11, Ssk2 and Ssk22) in response to osmotic stress. Ste11 or Ssk2 phosphorylates the MAPKK Pbs2 and then Pbs2 activates MAPK kinase Hog1 (Murakami *et al.*, 2008; Tatebayashi *et al.*, 2020). Furthermore, the MAPK cascades of AM fungus or host plants show the potential correlation to improve the resistance to drought tolerance (Huang *et al.*, 2020; Liu *et al.*, 2015b). However, there is no evidence to prove the causal relations between AM fungal and plant MAPK enhancing mycorrhizal plants' drought tolerance.

Although recent studies have revealed that AM fungus *Rhizophagus irregularis* possess many MAPK genes (Chen *et al.*, 2018; Tisserant *et al.*, 2013), relatively little is known about their precise roles in AM symbiosis and responding to external stresses, largely due to the difficulty in genetic manipulation of these obligate biotrophic fungi. VIGS is widely used to identify gene function with the advantages of short period and high efficiency (Chantreau *et al.*, 2015; Deng *et al.*, 2012). Host-induced gene silencing (HIGS) is developed based on the well-known RNA interference, which is to express double-strand RNA (dsRNA) of target gene in host plants. Research on pathogenic fungi using silencing of genes to improve plant resistance has been reported (Cheng *et al.*, 2015; Ghag *et al.*, 2014; Xu *et al.*, 2018). Moreover, VIGS and HIGS strategies were employed for functional studies of AM fungal genes during the *in planta* phase (Ezawa *et al.*, 2020; Hartmann *et al.*, 2020; Helber *et al.*, 2011; Xie *et al.*, 2016). Therefore, the powerful HIGS and VIGS techniques are two feasible strategies for the functional characterization of AM fungal genes during AM symbiosis.

Here, we report the positive responses of the plant *A. sinicus* to DS during AM symbiosis. We focus on the HOG1-MAPK cascade genes in the AM fungus *R. irregularis* DAOM197198. More importantly, we determine the biological functions of three HOG1-MAPK cascade genes (*RiSte11*, *RiPbs2* and *RiHog1*) of *R. irregularis* associated with host plant through both VIGS and HIGS strategies. Our findings reveal that AM fungus can improve host plant tolerance to drought through the HOG1-MAPK cascade of the fungal symbiont.

Results

Arbuscular mycorrhizal colonization enhances the *Astragalus sinicus* tolerance to drought stress

To estimate the role of arbuscular mycorrhiza in enhancing plant drought tolerance, the *A. sinicus* seedlings were colonized without (NM) or with (AM) *R. irregularis* under well water (WW) and DS conditions. The WW-treated pots contained 75% field water capacity (FWC), whereas the DS-treated pots contained 25% FWC. Our result showed that AM *A. sinicus* grew well, while the NM plants appeared with etiolated leaves (Figure S1a). It was found that *A. sinicus* roots formed arbuscular mycorrhiza after *R. irregularis* colonization (Figure S1b,c), while no AM fungal colonization was observed in NM roots (data not shown). And under the AM condition, there is no significant

difference in total colonization frequency (F%) and mycorrhization (M% and A%) between the WW and DS treatments (Figure S1d). Under both WW and DS conditions, the biomass of roots and shoots of AM *A. sinicus* was much higher than that of NM plants (Figure S1e,f). Particularly, under DS conditions, the fresh weight (FW) of AM roots is significantly higher than that of NM roots. Moreover, we found significant differences in the relative water content (RWC) and proline content of *A. sinicus* leaves between AM and NM plants under DS conditions. The data revealed that AM plants showed much higher RWC than NM plants, but significantly lower proline content than NM plants under DS conditions (Figure S1g,h). Proline is one of the most important physiological indicators for plants to cope with DS (Shrestha *et al.*, 2021). Overall, the above results indicated that AM fungal colonization significantly improved the mycorrhizal *A. sinicus* drought resistance under DS.

Identification of HOG1-MAPK cascade genes in *Rhizophagus irregularis*

Fungal MAPKs are essential for fungus–plant interaction subjected to DS (Huang *et al.*, 2020; Liu *et al.*, 2015b). Because among them the HOG1-MAPK cascade plays a critical role in the fungal osmoregulation (Román *et al.*, 2020; Wang *et al.*, 2021), we initiated a search for the HOG1-MAPK cascade genes in *R. irregularis*, using the related MAPK cascade genes in *S. cerevisiae* and other filamentous fungi as reference sequences (Hamel *et al.*, 2012). The *RiSte11*, *RiPbs2* and *RiHog1* from *R. irregularis* were identified by BLAST searches according to the released genome of *R. irregularis* strain DAOM 197198 (Chen *et al.*, 2018; Tisserant *et al.*, 2013). Results showed that the three candidate genes belong to the serine/threonine protein kinases MAPKKK, MAPKK and MAPK, respectively (Table S1). Further *in silico* analysis indicates that *RiSte11* contains 13 exons and 12 introns and encodes 690 amino acids, while *RiPbs2* contains 8 exons and 7 introns and encodes 351 amino acids; *RiHog1* contains 13 exons and 12 introns and encodes 359 amino acids (Figure S2a). The protein structure analysis reveals that *RiSte11* contains a SAM_Ste11_fungal (Sterile alpha motif) domain, a Ras_bdg-2 domain (The binding region of several Ser/Thr protein kinases) and a Serine/Threonine protein kinases domain, while both *RiPbs2* and *RiHog1* contain only one Serine/Threonine protein kinases domain (Figure S2b). Taken together, these *in silico* data showed that the HOG1-MAPK cascade in AM fungus *R. irregularis* is composed of the protein kinases *RiSte11*, *RiPbs2* and *RiHog1*.

HOG1-MAPK proteins from *Rhizophagus irregularis* are conserved across fungi species

To investigate the evolutionary relationships among *RiSte11*, *RiPbs2*, *RiHog1* and other members of the MAPK cascade proteins in AM and other fungal species, we performed a phylogenetic analysis that included 94 well-sequenced MAPK genes from diverse fungi. Based on sequence similarity, the fungal MAPK proteins tested could be divided into three groups: MAPKKK, MAPKK and MAPK. An unrooted phylogenetic tree shows the close relationship between *RiSte11*, *RiPbs2*, *RiHog1* and other AM fungal MAPK-related genes (Figure 1a). The MAPKKK group consists of Ste11-related proteins from different fungal species, while the *RiPbs2* protein from *R. irregularis* belongs to the MAPKK group. *RiSte11* and *RiPbs2* proteins are closely related to the Ste11 or Pbs2 among other AM fungal species. Moreover, the *RiHog1* protein belongs to the MAPK

Figure 1 The potential HOG1-MAPK cascade proteins in *Rhizophagus irregularis*. (a) Evolutionary relationships among *R. irregularis* RiSte11, RiPbs2, RiHog1 and related MAPK cascade proteins in other fungal species. The evolutionary history was inferred using MEGA7 software with the Neighbour-Joining method. Bootstrap values were calculated using 1000 replicates. RiSte11, RiPbs2 and RiHog1 proteins from *R. irregularis* are coloured in red. The bold branches represent the MAPK cascade proteins in other AM fungal species. (b–g) The predicted three-dimensional (3D) structures of *R. irregularis* RiSte11, RiPbs2 and RiHog1 proteins using the homologues derived from *Homo sapiens* ((b) 2xik.1.A; (d) 3w8q.1.A), *Arabidopsis thaliana* ((f) 5ci6.2.A) as templates, respectively. Arrows point out C-terminals and N-terminals. Homology modelling of the 3D structures of RiSte11, RiPbs2 and RiHog1 proteins were conducted with the Swiss Model program (<https://swissmodel.expasy.org/>).

three proteins may have the similarity in function with other HOG1-MAPK genes from other fungal species.

We further carried out homology modelling of RiSte11, RiPbs2 and RiHog1 proteins using *Homo sapiens* YSK1 (PDB-ID: 2xik.1.A), *Homo sapiens* MEK1 (3w8q.1.A) and *Arabidopsis thaliana* MPK6 (5ci6.2.A) as templates (Wang *et al.*, 2016), respectively. The predicted 3D models indicated that RiSte11, RiPbs2 and RiHog1 proteins were highly conserved compared with the MAPK-related proteins (templates) from their respective species (Figure 1b–g). Collectively, RiSte11, RiPbs2 and RiHog1 proteins are conserved across fungi species and closely relative to the AM fungi mitogen-activated protein kinases.

RiSte11, RiPbs2 and RiHog1 are expressed during the arbuscular mycorrhizal symbiosis

To determine whether the above functional predictions of RiSte11, RiPbs2 and RiHog1 have any physiological relevance, we first analysed the RNA-sequencing data of *RiSte11*, *RiPbs2* and *RiHog1* from *R. irregularis* transcriptomic databases (Morin *et al.*, 2019; Zeng *et al.*, 2018, 2020). The transcription of *RiSte11* in spores and mycorrhizal roots was higher than that in extraradical mycelium (ERM), while *RiPbs2* was uniformly expressed in spores, mycorrhizal roots and ERM. The transcription of *RiHog1* was slightly increased in spores and ERM compared with the mycorrhizal roots (Figure S3). Then the qRT-PCR was performed using cDNA from *A. sinicus* roots inoculated with *R. irregularis*. The results showed that transcripts of *RiSte11*, *RiPbs2* and *RiHog1* were also detectable in germinating spores, mycorrhizal *A. sinicus* roots (Myc-roots) and ERM. The transcription level of *RiSte11* in spores was almost twice that in ERM (Figure 2a). And as for *RiPbs2*, the expression difference among spores, Myc-roots and ERM were not obvious. While *RiHog1* was higher expressed in both spores and ERM than in Myc-roots (Figure 2b,c). The qRT-PCR results agree with the genomic analysis that these three genes are expressed in spores, mycorrhizal roots and ERM.

The results presented above prompted us to further determine the temporal expression of *RiSte11*, *RiPbs2* and *RiHog1* in mycorrhizal *A. sinicus* roots during different days post-inoculation (dpi). The transcripts of *RiSte11* and *RiPbs2* began to increase at 14 dpi, then kept increasing until 49 dpi (Figure 2d,e). While *RiHog1* transcripts showed a gradual increase trend from 14 to 56 dpi with AM fungal colonization (Figure 2f). We also analysed the expression levels of AM symbiotic marker genes *RiMST2* and *AsPT4* (Helber *et al.*, 2011; Xie *et al.*, 2013), which showed the expression of *RiMST2* and *AsPT4* kept increasing from 14 to 49 dpi (Figure 2g,h). During the later stage of symbiosis, higher expression levels of *RiSte11*, *RiPbs2* and *RiHog1* suggested that the three genes might play important roles in the physiological functions of mycorrhizal symbiosis. Taken together, our results from gene expression

analysis revealed that the HOG1-MAPK cascade genes in *R. irregularis* were induced during the *in planta* phase, suggesting that RiSte11, RiPbs2 and RiHog1 appear to be useful MAPKs that operate in the AM fungus *R. irregularis* crucial for the symbiotic relationship with plants.

RiSte11, RiPbs2 and RiHog1 are induced during the *in planta* phase in response to severe drought stress

To determine the effect of DS on the expression of *RiSte11*, *RiPbs2* and *RiHog1* during AM symbiosis, we performed a qRT-PCR analysis on the AM roots of *A. sinicus* plants exposed to different FWC. The results showed that DS caused weaker plant growth and plant leaves appeared etiolated (Figure S4a). Moreover, the severe DS led to the significantly decreased plant biomass, the lowered RWC and increased proline content in leaves (Figure S4b–d). Accordingly, the expression levels of HOG1-MAPK cascade genes in *R. irregularis* were also changed in response to different DSs. Both *RiSte11* and *RiHog1* showed elevated transcription levels in AM roots under severe DS (25% FWC) compared with the middle (50%FWC) and normal (75% FWC) water conditions, whereas *RiPbs2* exhibited an increased expression level in AM roots in the presence of the 25% FWC and 50% FWC (Figure 2i–k). The above results showed the transcription levels of *RiSte11*, *RiPbs2* and *RiHog1* increased significantly in mycorrhizal roots under severe DS, indicating that these three MAPKs may be manipulated by AM symbiosis for DS resistance.

Functional characterization of RiSte11, RiPbs2 and RiHog1 proteins in *Saccharomyces cerevisiae*

To determine whether the activity of RiSte11, RiPbs2 or RiHog1 modulates the growth of yeast cells in response to high osmotic stress, a complementation assay was performed with wild-type BY4741, $\Delta ste11$, $\Delta pbs2$ and $\Delta hog1$ yeast mutant. The empty pFL61 was used in the complementation assay, which carries the phosphoglycerate kinase promoter (PGK) separated by the terminator at *Not I* site in *S. cerevisiae* (Minet *et al.*, 1992). Sorbitol is widely used for simulating drought environment to verify yeast function (Li *et al.*, 2013), so the growth of the positive transformants was measured on synthetic dropout (SD/URA) medium and treated with different sorbitol concentrations. The result showed $\Delta ste11$ -pFL61, $\Delta pbs2$ -pFL61, $\Delta hog1$ -pFL61, $\Delta ste11$ -pFL61-RiSte11, $\Delta pbs2$ -pFL61-RiPbs2 and $\Delta hog1$ -pFL61-RiHog1 strains could grow as well as BY4741 strain with pFL61 on medium under standard condition. While under sorbitol condition, the $\Delta ste11$ -pFL61-RiSte11, $\Delta pbs2$ -pFL61-RiPbs2 and $\Delta hog1$ -pFL61-RiHog1 strains can complement the growth defect, but the $\Delta ste11$ strain expressing RiSte11 grow better than $\Delta ste11$ mutant under sorbitol treatment, and $\Delta pbs2$ and $\Delta hog1$ mutant could not survive well when given higher than 1 M sorbitol treatment (Figure 3a). The growth defects among $\Delta ste11$ -pFL61-RiSte11, $\Delta pbs2$ -pFL61-RiPbs2, $\Delta hog1$ -pFL61-

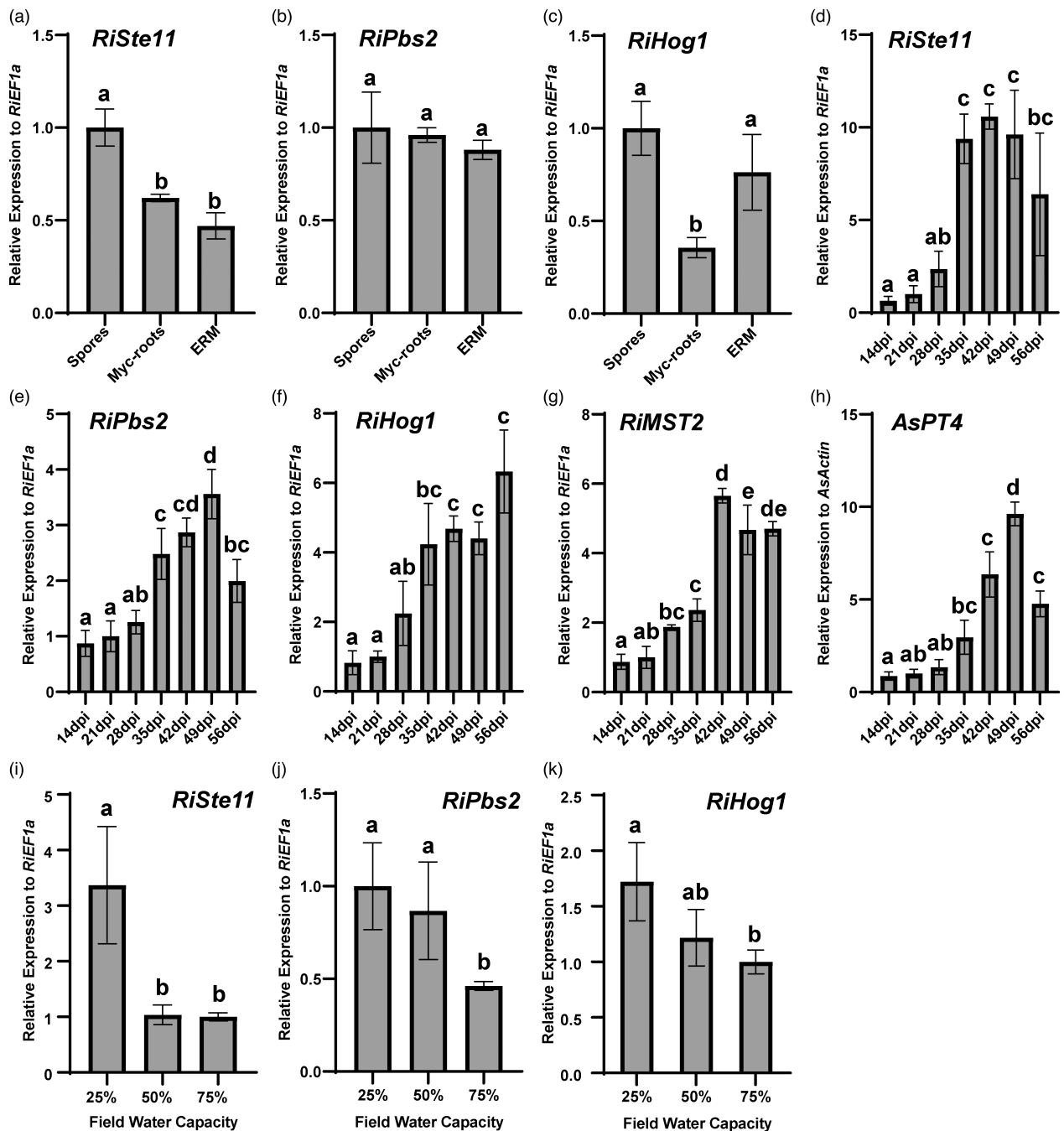


Figure 2 Expression patterns of *RiSte11*, *RiPbs2* and *RiHog1* from AM fungus *Rhizophagus irregularis*. (a–c) Expression levels of *RiSte11* (a), *RiPbs2* (b) and *RiHog1* (c) in different AM fungal tissues. Spores: germinating spores; Myc-roots: mycorrhizal *Astragalus sinicus* roots at 28 days post inoculation (dpi); ERM: extraradical mycelium. (d–h) Time-course analysis of the expression profiles of *RiSte11*, *RiPbs2*, *RiHog1*, *RiMST2* and *AsPT4* in *A. sinicus* roots at 14-, 21-, 28-, 35-, 42-, 49- and 56-days post inoculation (dpi) with *R. irregularis*. (i–k) Expression levels of *RiSte11*, *RiPbs2* and *RiHog1* from *R. irregularis* during the *in planta* phase at 42 dpi grown in 25%, 50% and 75% FWC. *RIEF1a* from *R. irregularis* and *A. sinicus* *AsActin* were used as reference genes for normalization. Error bars represent the means of three biological replicates with SE values, based on ANOVA-Tukey's test. The different letters indicate significant statistical differences between treatments at $P < 0.05$.

RiHog1, and $\Delta ste11$ -pFL61, $\Delta pbs2$ -pFL61, $\Delta hog1$ -pFL61 strains became gradually larger with sorbitol concentration increased (Figure 3b–g).

In yeast, trehalose is considered as a regulatory component to protect cells against various environmental stresses (Li et al., 2009). To examine the physiological roles of *RiSte11*, *RiPbs2* and *RiHog1*

in yeast cells under osmotic stress, we measured the trehalose content in the BY4741, $\Delta ste11$, $\Delta pbs2$, $\Delta hog1$ strains in response to 1 M sorbitol. As expected, the trehalose content in $\Delta ste11$ -pFL61-*RiSte11*, $\Delta pbs2$ -pFL61-*RiPbs2* and $\Delta hog1$ -pFL61-*RiHog1* strains were significantly higher than those in $\Delta ste11$, $\Delta pbs2$, $\Delta hog1$ carrying pFL61 under 1 M sorbitol condition. And the

trehalose content of the mutant strains expressing pFL61 was depressed in comparison with the control strain. While under standard conditions, the trehalose content of the $\Delta ste11$ -pFL61-*RiSte11*, $\Delta pbs2$ -pFL61-*RiPbs2* and $\Delta hog1$ -pFL61-*RiHog1* strains was not affected compared with the control (Figure 3h,i). The result indicated that $\Delta ste11$ expressing *RiSte11*, $\Delta pbs2$ expressing *RiPbs2* and $\Delta hog1$ expressing *RiHog1* can complement the defect under sorbitol treatment and enhance the yeast cells' resistance to osmotic stress.

To further determine subcellular localization of the *RiSte11*, *RiPbs2* and *RiHog1* kinases in yeast cells, each of the HOG1-MAPK genes was fused in-frame with GFP were placed into the vector pUG36 under the control of the *Adh-MET25* promoter. Confocal microscopy was conducted with the EY57 strain expressing each one of these three gene fusion constructs. The results showed that the GFP signals from all the three GFP-*RiSte11*, GFP-*RiPbs2* and GFP-*RiHog1* fusions displayed similar subcellular localization patterns that were in agreement with the free GFP cellular location under normal conditions. The result showed that the GFP signal from the pUG36-GFP free protein as a representative from this group was distributed throughout the cytoplasm and the nucleus of transformed cells (Figure 3j). Further subcellular localization analysis under osmotic stress (1 M sorbitol treatment) showed that GFP-*RiSte11* and GFP-*RiPbs2* were still localized throughout the cytoplasm, whereas the GFP-*RiHog1* fusion was predominantly localized in the nucleus, indicating that *RiHog1* may be localized both in the cytosol and the nucleus under standard conditions but predominately localized in the nucleus under osmotic stress. This result was further confirmed by the precise colocalization between GFP-*RiHog1* and the DAPI-labelled nucleus (Figure 3k). These findings indicated that *RiSte11* and *RiPbs2* proteins were mainly localized in the cytosol, while *RiHog1* protein was predominately localized to the nucleus in yeast cells during osmotic stress.

RiPbs2 interacts with RiSte11 or RiHog1 *in vitro*

It has been reported that the MAP kinase kinase *Pbs2* interact with the MAP kinase kinase *Ste11* or MAP kinase *Hog1* in yeast (Murakami *et al.*, 2008; Tatebayashi *et al.*, 2020). To investigate the potential interaction between *RiSte11* and *RiPbs2*, *RiPbs2* and *RiHog1* from *R. irregularis*, we conducted the pull-down assay *in vitro* using a prokaryotic expression system. We purified the *RiSte11*, *RiPbs2* and *RiHog1* as a recombinant MBP-*RiSte11*, GST-*RiPbs2*, HIS-*RiPbs2* and GST-*RiHog1* fusion protein from *Escherichia coli* BL21 (DE3). As expected, the result showed that GST-*RiPbs2* was pulled down by MBP-*RiSte11* at about 65 kDa and HIS-*RiPbs2* was pulled down by GST-*RiHog1* at about 55 kDa (Figure 4). This finding confirmed that *RiPbs2* interacts directly with *RiSte11* or *RiHog1* *in vitro*.

AM fungal HOG1-MAPK proteins (*RiSte11*, *RiPbs2* and *RiHog1*) facilitate plant drought resistance during arbuscular mycorrhizal symbiosis

To further investigate the biological functions of *R. irregularis* HOG1-MAPK cascade genes, we generated RNA interference (RNAi) constructs using the HIGS strategy. The *A. sinicus* plants with hairy roots were chosen as the host to perform the plant transformation, and the positive hairy roots with red fluorescence were observed (Figure S5). Then we planted the *A. sinicus* seedlings with transformed roots containing the *RiSte11-RNAi*, *RiPbs2-RNAi* or *RiHog1-RNAi* construct. The results showed that the AM-colonized *A. sinicus* plants grew significantly better than

NM plants under DS, whereas the silencing of *RiSte11*, *RiPbs2* or *RiHog1* in *R. irregularis* negatively affected the growth performance of mycorrhizal *A. sinicus* to drought resistance (Figure S6). We next estimated the RWC and proline content in control and RNAi plants. Lower levels of RWC were found in the leaves of *RiSte11-RNAi*, *RiPbs2-RNAi* or *RiHog1-RNAi* lines than in that of control lines. By contrast, higher levels of proline content were detected in the leaves of *RiSte11-RNAi*, *RiPbs2-RNAi* and *RiHog1-RNAi* lines in response to DS compared with control lines (Figure S7). To conform and extend the HIGS data, we further investigated the roles of *R. irregularis* HOG1-MAPK cascade genes upon AM symbiosis by the VIGS assay. In the VIGS experiment, the results showed that the changes in RWC and proline content in these VIGS-mediated silenced lines had a similar trend with that in the HIGS experiment. The level of RWC was lower but the proline content is higher in the *TRV2-RiSte11*, *TRV2-RiPbs2* or *TRV2-RiHog1* plants than that in control plants under DS (Figure S8). Overall, both HIGS and VIGS results revealed that AM fungal *RiSte11*, *RiPbs2* and *RiHog1* enhanced plant drought resistance during AM symbiosis.

Arbuscular mycorrhizal fungal HOG1-MAPK proteins (*RiSte11*, *RiPbs2* and *RiHog1*) are required for arbuscule development

To determine whether silencing of *RiSte11*, *RiPbs2* or *RiHog1* in *R. irregularis* affects the AM development under DS, we next estimated the role of *RiSte11*, *RiPbs2* or *RiHog1* in arbuscule development within plant roots. In the HIGS experiment, the expression levels of *RiSte11*, *RiPbs2* and *RiHog1* were decreased in *RiSte11-RNAi*, *RiPbs2-RNAi* or *RiHog1-RNAi* roots compared with in the control roots during DS (Figure 5a-c). The marker genes *AsPT4* and *RiMST2* also showed decreased expression in HIGS roots (Figure 5d,e). The total colonization frequency (F%) in most of *RiSte11-RNAi*, *RiPbs2-RNAi* or *RiHog1-RNAi* roots was slightly but not significantly lower than that in control lines, whereas the mycorrhiza intensity (M%) and arbuscule abundance (A%) of *RiSte11-RNAi* roots were reduced to average 32% and 15%, *RiPbs2-RNAi* roots were reduced to average 25% and 9%, *RiHog1-RNAi* roots were reduced to average 24% and 8%, respectively (Figure 5f-h). The arbuscules in control roots were mature with full branches. By contrast, most of the arbuscules in the *RiSte11-RNAi*, *RiPbs2-RNAi* and *RiHog1-RNAi* roots were severely collapsed or even dead (Figure 5i). The decreased abundance of arbuscules in the *RiSte11-RNAi* (or *RiPbs2-RNAi*, *RiHog1-RNAi*) lines was consistent with the expression levels of symbiotic marker genes *AsPT4* and *RiMST2* in *A. sinicus* and *R. irregularis*, respectively. Consistently, the expression levels and mycorrhizal colonization were also significantly reduced in the HIGS roots compared with the control roots under WW condition (Figure S9). This indicated that *RiSte11*, *RiPbs2* and *RiHog1* played a positive role in AM fungal root colonization.

In the VIGS experiment, the qRT-PCR was performed to estimate the transcripts of AM fungal *RiSte11*, *RiPbs2*, *RiHog1* and AM-specific marker genes *NbPT4* and *RiMST2* (Helber *et al.*, 2011; Wang *et al.*, 2018). Under DS, transcript levels of *RiSte11*, *RiPbs2* and *RiHog1* were significantly reduced in the *TRV2-RiSte11*, *TRV2-RiPbs2* and *TRV2-RiHog1* roots, respectively, compared with the control roots (Figure 6a-c). Similarly, the expression levels of *NbPT4* and *RiMST2* were repressed in *TRV2-RiSte11*, *TRV2-RiPbs2* and *TRV2-RiHog1* roots, respectively, in relative to the control roots (Figure 6d,e). There was no significant difference in F% between the VIGS and control roots. However,

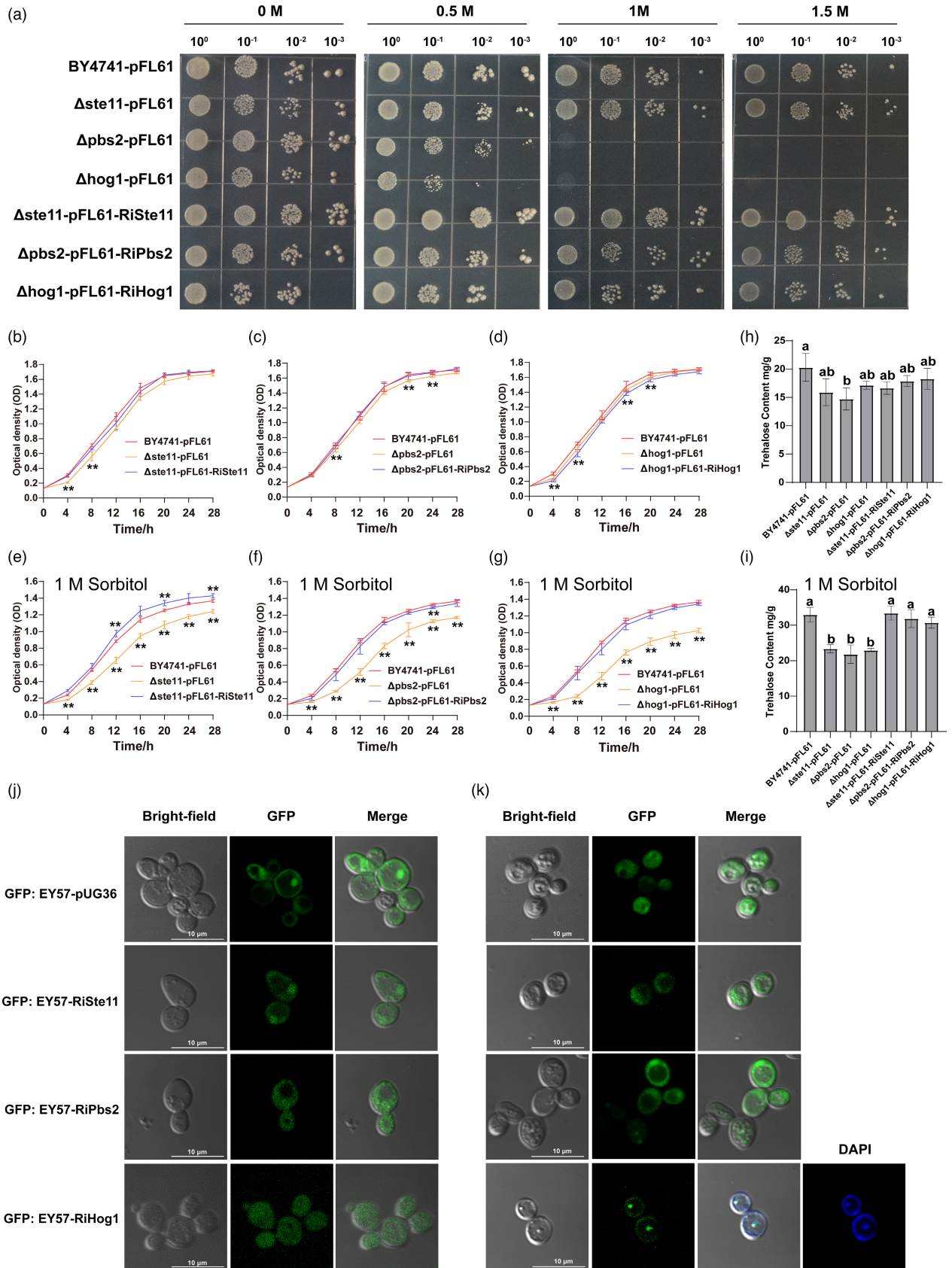


Figure 3 Functional characterization of RiSte11, RiPbs2 and RiHog1 in *Saccharomyces cerevisiae*. (a) Functional complementary analysis of yeast strains $\Delta ste11$, $\Delta pbs2$, $\Delta hog1$ expressing RiSte11, RiPbs2, RiHog1, respectively. They grow in the selective dropout (SD/-URA) medium containing different sorbitol concentrations. For the test, cells were grown to logarithmic phase and diluted to an OD₆₀₀ of 0.2, then ten-fold serial dilutions of cells were plated on the SD/-URA solid medium containing 0, 0.5, 1 or 1.5 M sorbitol, respectively. (b–g) Growth performances of $\Delta ste11$ -pFL61, $\Delta pbs2$ -pFL61, $\Delta hog1$ -pFL61, $\Delta ste11$ -pFL61-RiSte11, $\Delta pbs2$ -pFL61-RiPbs2, $\Delta hog1$ -pFL61-RiHog1 strains in the liquid medium containing 1 M sorbitol. The data represents the mean of three biological replicates \pm SE, based on ANOVA-Tukey's test. Asterisks showed the difference compared with the BY4751-pFL61 strain, * $P < 0.05$, ** $P < 0.01$. (h,i) Trehalose contents of transformed yeast BY4741 cells carrying pFL61, or complementary RiSte11, RiPbs2 or RiHog1 in response to non-sorbitol (h) or 1 M sorbitol (i). The data represents the mean of three biological replicates \pm SE, based on ANOVA-Tukey's test. The different letters indicate significant statistical differences between treatments at $P < 0.05$. (j–k) Subcellular localization of the free GFP (EY57-pUG36), GFP-RiSte11, GFP-RiPbs2 and GFP-RiHog1 fusions in yeast cells in response to standard growth conditions (j) or medium containing 1 M sorbitol (k). The bright-field views are exhibited in the left panels, while the GFP fluorescence images of each GFP-protein fusions are present in the middle panels. The blue fluorescence marker DAPI shows the position of the nucleus. The right panels indicate the bright-field and GFP or DAPI merged images. Scale bars, 10 μ m.

the *TRV2-RiSte11*, *TRV2-RiPbs2* and *TRV2-RiHog1* roots exhibited much lower M% and A% than the control roots (Figure 6f–h). The mature arbuscules were observed in the control roots, whereas the most arbuscules were severely impaired and collapsed (with many septa) in *TRV2-RiSte11*, *TRV2-RiPbs2* and *TRV2-RiHog1* roots (Figure 6i). And there was also a significant difference in AM development between the *TRV2-RiSte11*, *TRV2-RiPbs2*, *TRV2-RiHog1* and control lines under WW condition (Figure S10). Furthermore, based on the phylogenetic analysis of *A. thaliana* and other plants MAPKs (Chen *et al.*, 2021; Lin *et al.*, 1999), we found several MAPK-related genes in *Nicotiana benthamiana*, and they are named for *NbMAPK1*, *NbMAPK2*, *NbMAPK3*, *NbMAPK4*, *NbMAPK5*, *NbMAPK6*, *NbMAPK7*, *NbMAPK8*, *NbMAPK9*, *NbMAPK10*, *NbMAPK11*, *NbMAPK12*, *NbMAPK13*, *NbMAPK14*, *NbMAPK15*, *NbMAPK16*, *NbMAPK17*, *NbMAPK18*, *NbMAPK19*, *NbMAPK20*, *NbMAPK21*, *NbMAPK22*, *NbMAPK23*, *NbMAPK24*, *NbMAPK25*, *NbMAPK26*, *NbMAPK27*, *NbMAPK28*, *NbMAPK29*, *NbMAPK30*, *NbMAPK31*, *NbMAPK32*, *NbMAPK33*, *NbMAPK34*, *NbMAPK35*, *NbMAPK36*, *NbMAPK37*, *NbMAPK38*, *NbMAPK39*, *NbMAPK40*, *NbMAPK41*, *NbMAPK42*, *NbMAPK43*, *NbMAPK44*, *NbMAPK45*, *NbMAPK46*, *NbMAPK47*, *NbMAPK48*, *NbMAPK49*, *NbMAPK50*, *NbMAPK51*, *NbMAPK52*, *NbMAPK53*, *NbMAPK54*, *NbMAPK55*, *NbMAPK56*, *NbMAPK57*, *NbMAPK58*, *NbMAPK59*, *NbMAPK60*, *NbMAPK61*, *NbMAPK62*, *NbMAPK63*, *NbMAPK64*, *NbMAPK65*, *NbMAPK66*, *NbMAPK67*, *NbMAPK68*, *NbMAPK69*, *NbMAPK70*, *NbMAPK71*, *NbMAPK72*, *NbMAPK73*, *NbMAPK74*, *NbMAPK75*, *NbMAPK76*, *NbMAPK77*, *NbMAPK78*, *NbMAPK79*, *NbMAPK80*, *NbMAPK81*, *NbMAPK82*, *NbMAPK83*, *NbMAPK84*, *NbMAPK85*, *NbMAPK86*, *NbMAPK87*, *NbMAPK88*, *NbMAPK89*, *NbMAPK90*, *NbMAPK91*, *NbMAPK92*, *NbMAPK93*, *NbMAPK94*, *NbMAPK95*, *NbMAPK96*, *NbMAPK97*, *NbMAPK98*, *NbMAPK99*, *NbMAPK100*, *NbMAPK101*, *NbMAPK102*, *NbMAPK103*, *NbMAPK104*, *NbMAPK105*, *NbMAPK106*, *NbMAPK107*, *NbMAPK108*, *NbMAPK109*, *NbMAPK110*, *NbMAPK111*, *NbMAPK112*, *NbMAPK113*, *NbMAPK114*, *NbMAPK115*, *NbMAPK116*, *NbMAPK117*, *NbMAPK118*, *NbMAPK119*, *NbMAPK120*, *NbMAPK121*, *NbMAPK122*, *NbMAPK123*, *NbMAPK124*, *NbMAPK125*, *NbMAPK126*, *NbMAPK127*, *NbMAPK128*, *NbMAPK129*, *NbMAPK130*, *NbMAPK131*, *NbMAPK132*, *NbMAPK133*, *NbMAPK134*, *NbMAPK135*, *NbMAPK136*, *NbMAPK137*, *NbMAPK138*, *NbMAPK139*, *NbMAPK140*, *NbMAPK141*, *NbMAPK142*, *NbMAPK143*, *NbMAPK144*, *NbMAPK145*, *NbMAPK146*, *NbMAPK147*, *NbMAPK148*, *NbMAPK149*, *NbMAPK150*, *NbMAPK151*, *NbMAPK152*, *NbMAPK153*, *NbMAPK154*, *NbMAPK155*, *NbMAPK156*, *NbMAPK157*, *NbMAPK158*, *NbMAPK159*, *NbMAPK160*, *NbMAPK161*, *NbMAPK162*, *NbMAPK163*, *NbMAPK164*, *NbMAPK165*, *NbMAPK166*, *NbMAPK167*, *NbMAPK168*, *NbMAPK169*, *NbMAPK170*, *NbMAPK171*, *NbMAPK172*, *NbMAPK173*, *NbMAPK174*, *NbMAPK175*, *NbMAPK176*, *NbMAPK177*, *NbMAPK178*, *NbMAPK179*, *NbMAPK180*, *NbMAPK181*, *NbMAPK182*, *NbMAPK183*, *NbMAPK184*, *NbMAPK185*, *NbMAPK186*, *NbMAPK187*, *NbMAPK188*, *NbMAPK189*, *NbMAPK190*, *NbMAPK191*, *NbMAPK192*, *NbMAPK193*, *NbMAPK194*, *NbMAPK195*, *NbMAPK196*, *NbMAPK197*, *NbMAPK198*, *NbMAPK199*, *NbMAPK200*, *NbMAPK201*, *NbMAPK202*, *NbMAPK203*, *NbMAPK204*, *NbMAPK205*, *NbMAPK206*, *NbMAPK207*, *NbMAPK208*, *NbMAPK209*, *NbMAPK210*, *NbMAPK211*, *NbMAPK212*, *NbMAPK213*, *NbMAPK214*, *NbMAPK215*, *NbMAPK216*, *NbMAPK217*, *NbMAPK218*, *NbMAPK219*, *NbMAPK220*, *NbMAPK221*, *NbMAPK222*, *NbMAPK223*, *NbMAPK224*, *NbMAPK225*, *NbMAPK226*, *NbMAPK227*, *NbMAPK228*, *NbMAPK229*, *NbMAPK230*, *NbMAPK231*, *NbMAPK232*, *NbMAPK233*, *NbMAPK234*, *NbMAPK235*, *NbMAPK236*, *NbMAPK237*, *NbMAPK238*, *NbMAPK239*, *NbMAPK240*, *NbMAPK241*, *NbMAPK242*, *NbMAPK243*, *NbMAPK244*, *NbMAPK245*, *NbMAPK246*, *NbMAPK247*, *NbMAPK248*, *NbMAPK249*, *NbMAPK250*, *NbMAPK251*, *NbMAPK252*, *NbMAPK253*, *NbMAPK254*, *NbMAPK255*, *NbMAPK256*, *NbMAPK257*, *NbMAPK258*, *NbMAPK259*, *NbMAPK260*, *NbMAPK261*, *NbMAPK262*, *NbMAPK263*, *NbMAPK264*, *NbMAPK265*, *NbMAPK266*, *NbMAPK267*, *NbMAPK268*, *NbMAPK269*, *NbMAPK270*, *NbMAPK271*, *NbMAPK272*, *NbMAPK273*, *NbMAPK274*, *NbMAPK275*, *NbMAPK276*, *NbMAPK277*, *NbMAPK278*, *NbMAPK279*, *NbMAPK280*, *NbMAPK281*, *NbMAPK282*, *NbMAPK283*, *NbMAPK284*, *NbMAPK285*, *NbMAPK286*, *NbMAPK287*, *NbMAPK288*, *NbMAPK289*, *NbMAPK290*, *NbMAPK291*, *NbMAPK292*, *NbMAPK293*, *NbMAPK294*, *NbMAPK295*, *NbMAPK296*, *NbMAPK297*, *NbMAPK298*, *NbMAPK299*, *NbMAPK300*, *NbMAPK301*, *NbMAPK302*, *NbMAPK303*, *NbMAPK304*, *NbMAPK305*, *NbMAPK306*, *NbMAPK307*, *NbMAPK308*, *NbMAPK309*, *NbMAPK310*, *NbMAPK311*, *NbMAPK312*, *NbMAPK313*, *NbMAPK314*, *NbMAPK315*, *NbMAPK316*, *NbMAPK317*, *NbMAPK318*, *NbMAPK319*, *NbMAPK320*, *NbMAPK321*, *NbMAPK322*, *NbMAPK323*, *NbMAPK324*, *NbMAPK325*, *NbMAPK326*, *NbMAPK327*, *NbMAPK328*, *NbMAPK329*, *NbMAPK330*, *NbMAPK331*, *NbMAPK332*, *NbMAPK333*, *NbMAPK334*, *NbMAPK335*, *NbMAPK336*, *NbMAPK337*, *NbMAPK338*, *NbMAPK339*, *NbMAPK340*, *NbMAPK341*, *NbMAPK342*, *NbMAPK343*, *NbMAPK344*, *NbMAPK345*, *NbMAPK346*, *NbMAPK347*, *NbMAPK348*, *NbMAPK349*, *NbMAPK350*, *NbMAPK351*, *NbMAPK352*, *NbMAPK353*, *NbMAPK354*, *NbMAPK355*, *NbMAPK356*, *NbMAPK357*, *NbMAPK358*, *NbMAPK359*, *NbMAPK360*, *NbMAPK361*, *NbMAPK362*, *NbMAPK363*, *NbMAPK364*, *NbMAPK365*, *NbMAPK366*, *NbMAPK367*, *NbMAPK368*, *NbMAPK369*, *NbMAPK370*, *NbMAPK371*, *NbMAPK372*, *NbMAPK373*, *NbMAPK374*, *NbMAPK375*, *NbMAPK376*, *NbMAPK377*, *NbMAPK378*, *NbMAPK379*, *NbMAPK380*, *NbMAPK381*, *NbMAPK382*, *NbMAPK383*, *NbMAPK384*, *NbMAPK385*, *NbMAPK386*, *NbMAPK387*, *NbMAPK388*, *NbMAPK389*, *NbMAPK390*, *NbMAPK391*, *NbMAPK392*, *NbMAPK393*, *NbMAPK394*, *NbMAPK395*, *NbMAPK396*, *NbMAPK397*, *NbMAPK398*, *NbMAPK399*, *NbMAPK400*, *NbMAPK401*, *NbMAPK402*, *NbMAPK403*, *NbMAPK404*, *NbMAPK405*, *NbMAPK406*, *NbMAPK407*, *NbMAPK408*, *NbMAPK409*, *NbMAPK410*, *NbMAPK411*, *NbMAPK412*, *NbMAPK413*, *NbMAPK414*, *NbMAPK415*, *NbMAPK416*, *NbMAPK417*, *NbMAPK418*, *NbMAPK419*, *NbMAPK420*, *NbMAPK421*, *NbMAPK422*, *NbMAPK423*, *NbMAPK424*, *NbMAPK425*, *NbMAPK426*, *NbMAPK427*, *NbMAPK428*, *NbMAPK429*, *NbMAPK430*, *NbMAPK431*, *NbMAPK432*, *NbMAPK433*, *NbMAPK434*, *NbMAPK435*, *NbMAPK436*, *NbMAPK437*, *NbMAPK438*, *NbMAPK439*, *NbMAPK440*, *NbMAPK441*, *NbMAPK442*, *NbMAPK443*, *NbMAPK444*, *NbMAPK445*, *NbMAPK446*, *NbMAPK447*, *NbMAPK448*, *NbMAPK449*, *NbMAPK450*, *NbMAPK451*, *NbMAPK452*, *NbMAPK453*, *NbMAPK454*, *NbMAPK455*, *NbMAPK456*, *NbMAPK457*, *NbMAPK458*, *NbMAPK459*, *NbMAPK460*, *NbMAPK461*, *NbMAPK462*, *NbMAPK463*, *NbMAPK464*, *NbMAPK465*, *NbMAPK466*, *NbMAPK467*, *NbMAPK468*, *NbMAPK469*, *NbMAPK470*, *NbMAPK471*, *NbMAPK472*, *NbMAPK473*, *NbMAPK474*, *NbMAPK475*, *NbMAPK476*, *NbMAPK477*, *NbMAPK478*, *NbMAPK479*, *NbMAPK480*, *NbMAPK481*, *NbMAPK482*, *NbMAPK483*, *NbMAPK484*, *NbMAPK485*, *NbMAPK486*, *NbMAPK487*, *NbMAPK488*, *NbMAPK489*, *NbMAPK490*, *NbMAPK491*, *NbMAPK492*, *NbMAPK493*, *NbMAPK494*, *NbMAPK495*, *NbMAPK496*, *NbMAPK497*, *NbMAPK498*, *NbMAPK499*, *NbMAPK500*, *NbMAPK501*, *NbMAPK502*, *NbMAPK503*, *NbMAPK504*, *NbMAPK505*, *NbMAPK506*, *NbMAPK507*, *NbMAPK508*, *NbMAPK509*, *NbMAPK510*, *NbMAPK511*, *NbMAPK512*, *NbMAPK513*, *NbMAPK514*, *NbMAPK515*, *NbMAPK516*, *NbMAPK517*, *NbMAPK518*, *NbMAPK519*, *NbMAPK520*, *NbMAPK521*, *NbMAPK522*, *NbMAPK523*, *NbMAPK524*, *NbMAPK525*, *NbMAPK526*, *NbMAPK527*, *NbMAPK528*, *NbMAPK529*, *NbMAPK530*, *NbMAPK531*, *NbMAPK532*, *NbMAPK533*, *NbMAPK534*, *NbMAPK535*, *NbMAPK536*, *NbMAPK537*, *NbMAPK538*, *NbMAPK539*, *NbMAPK540*, *NbMAPK541*, *NbMAPK542*, *NbMAPK543*, *NbMAPK544*, *NbMAPK545*, *NbMAPK546*, *NbMAPK547*, *NbMAPK548*, *NbMAPK549*, *NbMAPK550*, *NbMAPK551*, *NbMAPK552*, *NbMAPK553*, *NbMAPK554*, *NbMAPK555*, *NbMAPK556*, *NbMAPK557*, *NbMAPK558*, *NbMAPK559*, *NbMAPK560*, *NbMAPK561*, *NbMAPK562*, *NbMAPK563*, *NbMAPK564*, *NbMAPK565*, *NbMAPK566*, *NbMAPK567*, *NbMAPK568*, *NbMAPK569*, *NbMAPK570*, *NbMAPK571*, *NbMAPK572*, *NbMAPK573*, *NbMAPK574*, *NbMAPK575*, *NbMAPK576*, *NbMAPK577*, *NbMAPK578*, *NbMAPK579*, *NbMAPK580*, *NbMAPK581*, *NbMAPK582*, *NbMAPK583*, *NbMAPK584*, *NbMAPK585*, *NbMAPK586*, *NbMAPK587*, *NbMAPK588*, *NbMAPK589*, *NbMAPK590*, *NbMAPK591*, *NbMAPK592*, *NbMAPK593*, *NbMAPK594*, *NbMAPK595*, *NbMAPK596*, *NbMAPK597*, *NbMAPK598*, *NbMAPK599*, *NbMAPK600*, *NbMAPK601*, *NbMAPK602*, *NbMAPK603*, *NbMAPK604*, *NbMAPK605*, *NbMAPK606*, *NbMAPK607*, *NbMAPK608*, *NbMAPK609*, *NbMAPK610*, *NbMAPK611*, *NbMAPK612*, *NbMAPK613*, *NbMAPK614*, *NbMAPK615*, *NbMAPK616*, *NbMAPK617*, *NbMAPK618*, *NbMAPK619*, *NbMAPK620*, *NbMAPK621*, *NbMAPK622*, *NbMAPK623*, *NbMAPK624*, *NbMAPK625*, *NbMAPK626*, *NbMAPK627*, *NbMAPK628*, *NbMAPK629*, *NbMAPK630*, *NbMAPK631*, *NbMAPK632*, *NbMAPK633*, *NbMAPK634*, *NbMAPK635*, *NbMAPK636*, *NbMAPK637*, *NbMAPK638*, *NbMAPK639*, *NbMAPK640*, *NbMAPK641*, *NbMAPK642*, *NbMAPK643*, *NbMAPK644*, *NbMAPK645*, *NbMAPK646*, *NbMAPK647*, *NbMAPK648*, *NbMAPK649*, *NbMAPK650*, *NbMAPK651*, *NbMAPK652*, *NbMAPK653*, *NbMAPK654*, *NbMAPK655*, *NbMAPK656*, *NbMAPK657*, *NbMAPK658*, *NbMAPK659*, *NbMAPK660*, *NbMAPK661*, *NbMAPK662*, *NbMAPK663*, *NbMAPK664*, *NbMAPK665*, *NbMAPK666*, *NbMAPK667*, *NbMAPK668*, *NbMAPK669*, *NbMAPK670*, *NbMAPK671*, *NbMAPK672*, *NbMAPK673*, *NbMAPK674*, *NbMAPK675*, *NbMAPK676*, *NbMAPK677*, *NbMAPK678*, *NbMAPK679*, *NbMAPK680*, *NbMAPK681*, *NbMAPK682*, *NbMAPK683*, *NbMAPK684*, *NbMAPK685*, *NbMAPK686*, *NbMAPK687*, *NbMAPK688*, *NbMAPK689*, *NbMAPK690*, *NbMAPK691*, *NbMAPK692*, *NbMAPK693*, *NbMAPK694*, *NbMAPK695*, *NbMAPK696*, *NbMAPK697*, *NbMAPK698*, *NbMAPK699*, *NbMAPK700*, *NbMAPK701*, *NbMAPK702*, *NbMAPK703*, *NbMAPK704*, *NbMAPK705*, *NbMAPK706*, *NbMAPK707*, *NbMAPK708*, *NbMAPK709*, *NbMAPK710*, *NbMAPK711*, *NbMAPK712*, *NbMAPK713*, *NbMAPK714*, *NbMAPK715*, *NbMAPK716*, *NbMAPK717*, *NbMAPK718*, *NbMAPK719*, *NbMAPK720*, *NbMAPK721*, *NbMAPK722*, *NbMAPK723*, *NbMAPK724*, *NbMAPK725*, *NbMAPK726*, *NbMAPK727*, *NbMAPK728*, *NbMAPK729*, *NbMAPK730*, *NbMAPK731*, *NbMAPK732*, *NbMAPK733*, *NbMAPK734*, *NbMAPK735*, *NbMAPK736*, *NbMAPK737*, *NbMAPK738*, *NbMAPK739*, *NbMAPK740*, *NbMAPK741*, *NbMAPK742*, *NbMAPK743*, *NbMAPK744*, *NbMAPK745*, *NbMAPK746*, *NbMAPK747*, *NbMAPK748*, *NbMAPK749*, *NbMAPK750*, *NbMAPK751*, *NbMAPK752*, *NbMAPK753*, *NbMAPK754*, *NbMAPK755*, *NbMAPK756*, *NbMAPK757*, *NbMAPK758*, *NbMAPK759*, *NbMAPK760*, *NbMAPK761*, *NbMAPK762*, *NbMAPK763*, *NbMAPK764*, *NbMAPK765*, *NbMAPK766*, *NbMAPK767*, *NbMAPK768*, *NbMAPK769*, *NbMAPK770*, *NbMAPK771*, *NbMAPK772*, *NbMAPK773*, *NbMAPK774*, *NbMAPK775*, *NbMAPK776*, *NbMAPK777*, *NbMAPK778*, *NbMAPK779*, *NbMAPK780*, *NbMAPK781*, *NbMAPK782*, *NbMAPK783*, *NbMAPK784*, *NbMAPK785*, *NbMAPK786*, *NbMAPK787*, *NbMAPK788*, *NbMAPK789*, *NbMAPK790*, *NbMAPK791*, *NbMAPK792*, *NbMAPK793*, *NbMAPK794*, *NbMAPK795*, *NbMAPK796*, *NbMAPK797*, *NbMAPK798*, *NbMAPK799*, *NbMAPK800*, *NbMAPK801*, *NbMAPK802*, *NbMAPK803*, *NbMAPK804*, *NbMAPK805*, *NbMAPK806*, *NbMAPK807*, *NbMAPK808*, *NbMAPK809*, *NbMAPK810*, *NbMAPK811*, *NbMAPK812*, *NbMAPK813*, *NbMAPK814*, *NbMAPK815*, *NbMAPK816*, *NbMAPK817*, *NbMAPK818*, *NbMAPK819*, *NbMAPK820*, *NbMAPK821*, *NbMAPK822*, *NbMAPK823*, *NbMAPK824*, *NbMAPK825*, *NbMAPK826*, *NbMAPK827*, *NbMAPK828*, *NbMAPK829*, *NbMAPK830*, *NbMAPK831*, *NbMAPK832*, *NbMAPK833*, *NbMAPK834*, *NbMAPK835*, *NbMAPK836*, *NbMAPK837*, *NbMAPK838*, *NbMAPK839*, *NbMAPK840*, *NbMAPK841*, *NbMAPK842*, *NbMAPK843*, *NbMAPK844*, *NbMAPK845*, *NbMAPK846*, *NbMAPK847*, *NbMAPK848*, *NbMAPK849*, *NbMAPK850*, *NbMAPK851*, *NbMAPK852*, *NbMAPK853*, *NbMAPK854*, *NbMAPK855*, *NbMAPK856*, *NbMAPK857*, *NbMAPK858*, *NbMAPK859*, *NbMAPK860*, *NbMAPK861*, *NbMAPK862*, *NbMAPK863*, *NbMAPK864*, *NbMAPK865*, *NbMAPK866*, *NbMAPK867*, *NbMAPK868*, *NbMAPK869*, *NbMAPK870*, *NbMAPK871*, *NbMAPK872*, *NbMAPK873*, *NbMAPK874*, *NbMAPK875*, *NbMAPK876*, *NbMAPK877*, *NbMAPK878*, *NbMAPK879*, *NbMAPK880*, *NbMAPK881*, *NbMAPK882*, *NbMAPK883*, *NbMAPK884*, *NbMAPK885*, *NbMAPK886*, *NbMAPK887*, *NbMAPK888*, *NbMAPK889*, *NbMAPK890*, *NbMAPK891*, *NbMAPK892*, *NbMAPK893*, *NbMAPK894*, *NbMAPK895*, *NbMAPK896*, *NbMAPK897*, *NbMAPK898*, *NbMAPK899*, *NbMAPK900*, *NbMAPK901*, *NbMAPK902*, *NbMAPK903*, *NbMAPK904*, *NbMAPK905*, *NbMAPK906*, *NbMAPK907*, *NbMAPK908*, *NbMAPK909*, *NbMAPK910*, *NbMAPK911*, *NbMAPK912*, *NbMAPK913*, *NbMAPK914*, *NbMAPK915*, *NbMAPK916*, *NbMAPK917*, *NbMAPK918*, *NbMAPK919*, *NbMAPK920*, *NbMAPK921*, *NbMAPK922*, *NbMAPK923*, *NbMAPK924*, *NbMAPK925*, *NbMAPK926*, *NbMAPK927*, *NbMAPK928*, *NbMAPK929*, *NbMAPK930*, *NbMAPK931*, *NbMAPK932*, *NbMAPK933*, *NbMAPK934*, *NbMAPK935*, *NbMAPK936*, *NbMAPK937*, *NbMAPK938*, *NbMAPK939*, *NbMAPK940*, *NbMAPK941*, *NbMAPK942*, *NbMAPK943*, *NbMAPK944*, *NbMAPK945*, *NbMAPK946*, *NbMAPK947*, *NbMAPK948*, *NbMAPK949*, *NbMAPK950*, *NbMAPK951*, *NbMAPK952*, *NbMAPK953*, *NbMAPK954*

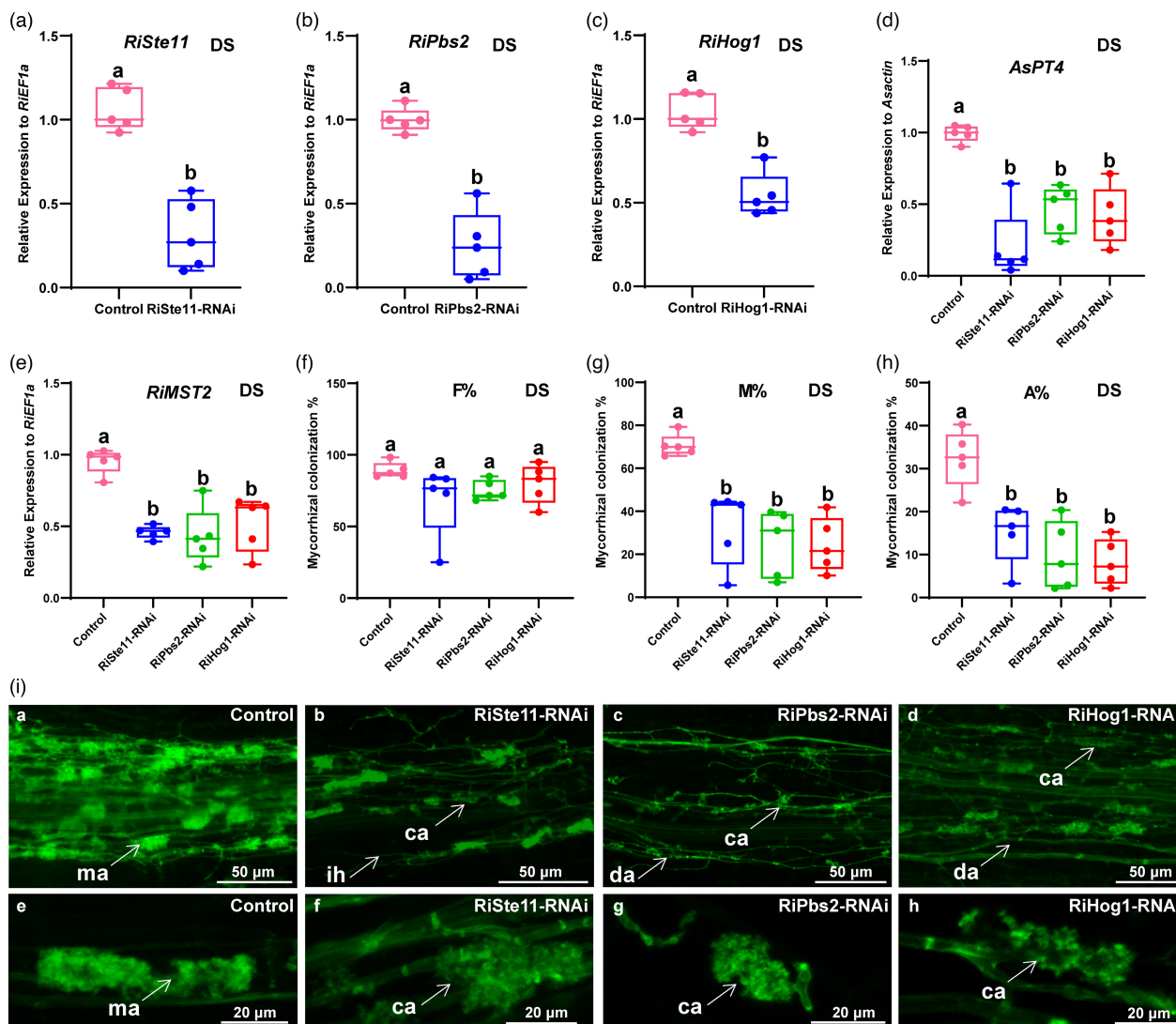


Figure 5 Host-induced gene silencing of HOG1-MAPK cascade genes in *Rhizophagus irregularis* inhibits arbuscule development in roots under drought stress. (a–h) Expression levels of *R. irregularis* *RiSte11* (a), *RiPbs2* (b), *RiHog1* (c), symbiosis-specific marker genes *AsPT4* (d) and *RiMST2* (e) in control and *RiSte11*-RNAi, *RiPbs2*-RNAi or *RiHog1*-RNAi lines. *A. sinicus* *AsActin* and *R. irregularis* *RIEF1a* genes were used as the reference genes for normalization, respectively. (f–h) Mycorrhizal colonization levels in control and *RiSte11*-RNAi, *RiPbs2*-RNAi or *RiHog1*-RNAi roots with *R. irregularis* after the WGA488 staining. F%, total frequency of colonization; M%, intensity of mycorrhiza; A%, arbuscule abundance. Error bars represent the means of five biological replicates with SE values. The different letters indicate significant statistical differences between treatments at $P < 0.05$, based on one-way ANOVA, Tukey's test. (i) Laser-scanning confocal microscopy images of *R. irregularis* in control and *RiSte11*-RNAi, *RiPbs2*-RNAi or *RiHog1*-RNAi roots after the WGA488 staining. ma, mature arbuscules; ca, collapsed arbuscule; da, degenerating arbuscules; ih, intraradical hyphae. Scale bars are shown in the images.

Discussion

It has been affirmed that AM fungi can alleviate the negative effects of drought by regulating plant physiological and molecular responses (Püschel et al., 2021; Zhang et al., 2020). Our results also confirmed that AM symbiosis has the ability to improve host performance under DS. As a result, mycorrhizal plants might acquire more nutrition and promote the transport of water exposed to DS (Gholamhoseini et al., 2013; Hazzoumi et al., 2015; Hu et al., 2020; Leyva-Morales et al., 2019). Fungal MAPK cascades serve as protein kinases, which have significant importance in connecting external stress signals with cellular responses and downstream gene expression (Kou and Naqvi, 2016). In this study, we investigated the biological

functions of HOG1-MAPK cascade genes that operated in *R. irregularis* during AM symbiosis under DS.

Many studies have shown that plant MAPK cascade improves plant drought resistance (Zhu et al., 2020, 2021), but the mechanism of AM fungal MAPK cascade in promoting plant drought resistance is rarely reported. Although recent studies show the potential correlation between AM fungal and plants MAPK cascades (Huang et al., 2020; Liu et al., 2015b), there is no evidence to prove the causal relations between AM fungal and plant MAPK enhancing mycorrhizal plants' drought tolerance. These allowed us to propose that AM fungi might regulate the plant drought-stress response through the activation of MAPK proteins. The HOG1-MAPK cascade is conserved in fungi including yeast and other pathogenic fungi to activate responses to

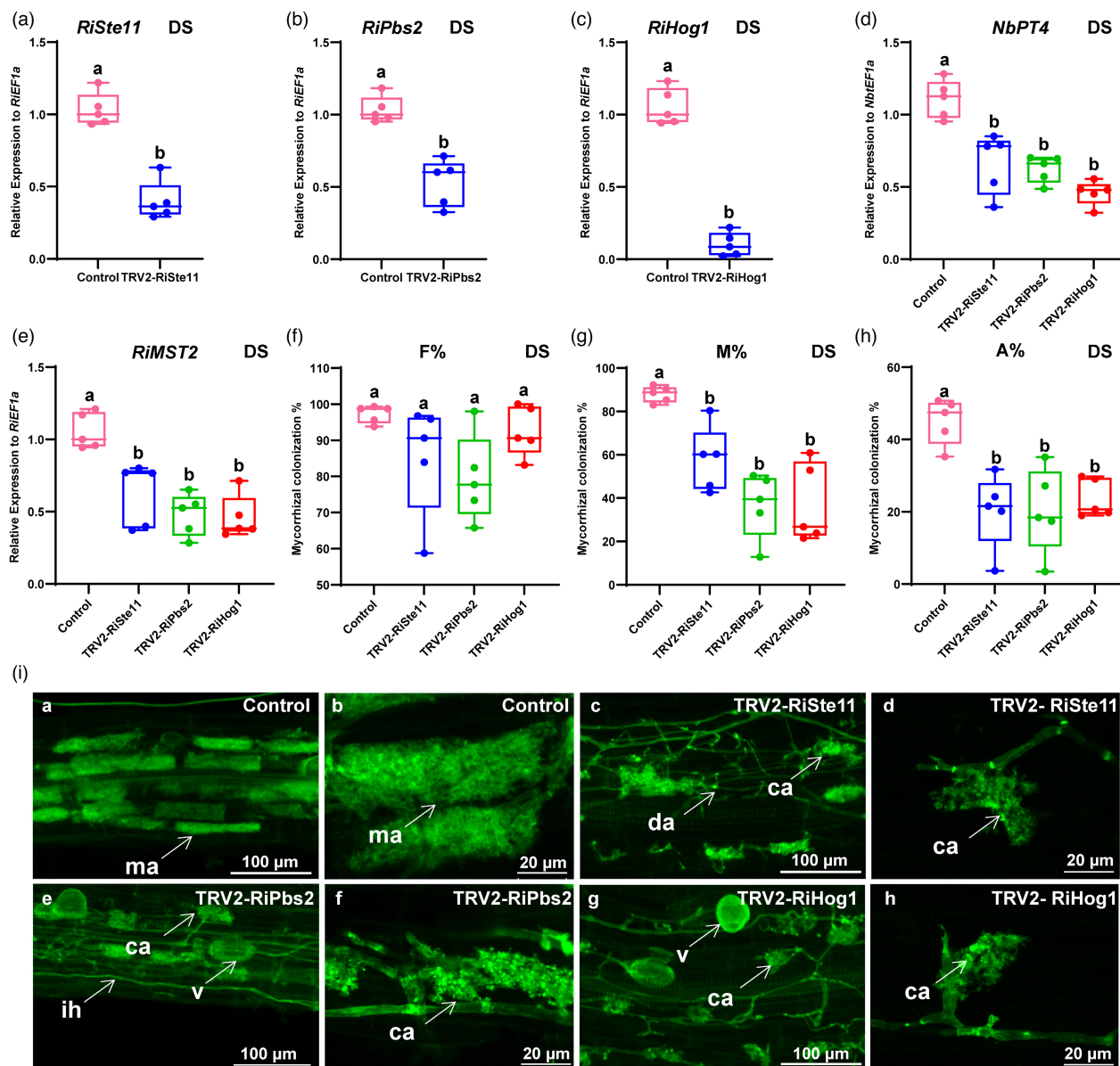


Figure 6 Molecular and arbuscular mycorrhizal phenotypes of virus-induced gene silencing of *RiSte11*, *RiPbs2* or *RiHog1* in *Nicotiana benthamiana* under drought stress. Expression levels of *RiSte11* (a), *RiPbs2* (b), *RiHog1* (c), symbiosis-specific marker genes *NbPT4* (d) and *RiMST2* (e) in control and TRV2-*RiSte11*, TRV2-*RiPbs2* or TRV2-*RiHog1* roots with *Rhizophagus irregularis*. The *N. benthamiana* *NbtEF1a* and *R. irregularis* *RiEF1a* genes were used as the reference genes for normalization, respectively. (f–h) Mycorrhization colonization levels of the control and *RiSte11*-silenced (TRV2-*RiSte11*), *RiPbs2*-silenced (TRV2-*RiPbs2*) or *RiHog1*-silenced (TRV2-*RiHog1*) *N. benthamiana* roots with *R. irregularis*. F%, total frequency of colonization; M%, intensity of mycorrhiza; A%, arbuscule abundance. Error bars represent the means of five biological replicates \pm SE. The different letters indicate significant statistical differences between treatments at $P < 0.05$, based on one-way ANOVA, Tukey's test. i. Arbuscule phenotype of *R. irregularis* in control and TRV2-*RiSte11*, TRV2-*RiPbs2* or TRV2-*RiHog1* roots after the WGA488 staining. ca, collapsed arbuscule; da, degenerating arbuscules; ih, intraradical hyphae; ma, mature arbuscules; v, vesicle. Scale bars are as shown in the images.

different stress signals (Hamel *et al.*, 2012). We found the three HOG1-MAPK cascades (*RiSte11*, *RiPbs2* and *RiHog1*) had similarities with other known HOG1-MAPK homologues from closely related fungal species. These indicated the HOG1-MAPK cascade may have a similar function across fungal species that respond to abiotic stress (Martínez-Soto and Ruiz-Herrera, 2017). The development of AM symbiosis consists of different stages through the progression of AM fungal hyphae during root colonization

(Parniske, 2008). During arbuscule formation, the hypha enters the root and grows into the cortex cells where arbuscules was established (Gutjahr and Parniske, 2013; Harrison, 2012). Arbuscules are considered to be the primary sites for nutrient exchange between the host and AM fungi (Bonfante and Genre, 2010). Our study also showed that *RiSte11*, *RiPbs2* and *RiHog1* genes were expressed during the *in planta* phase. Based on these findings, we propose that HOG1-MAPK cascade may regulate plants'

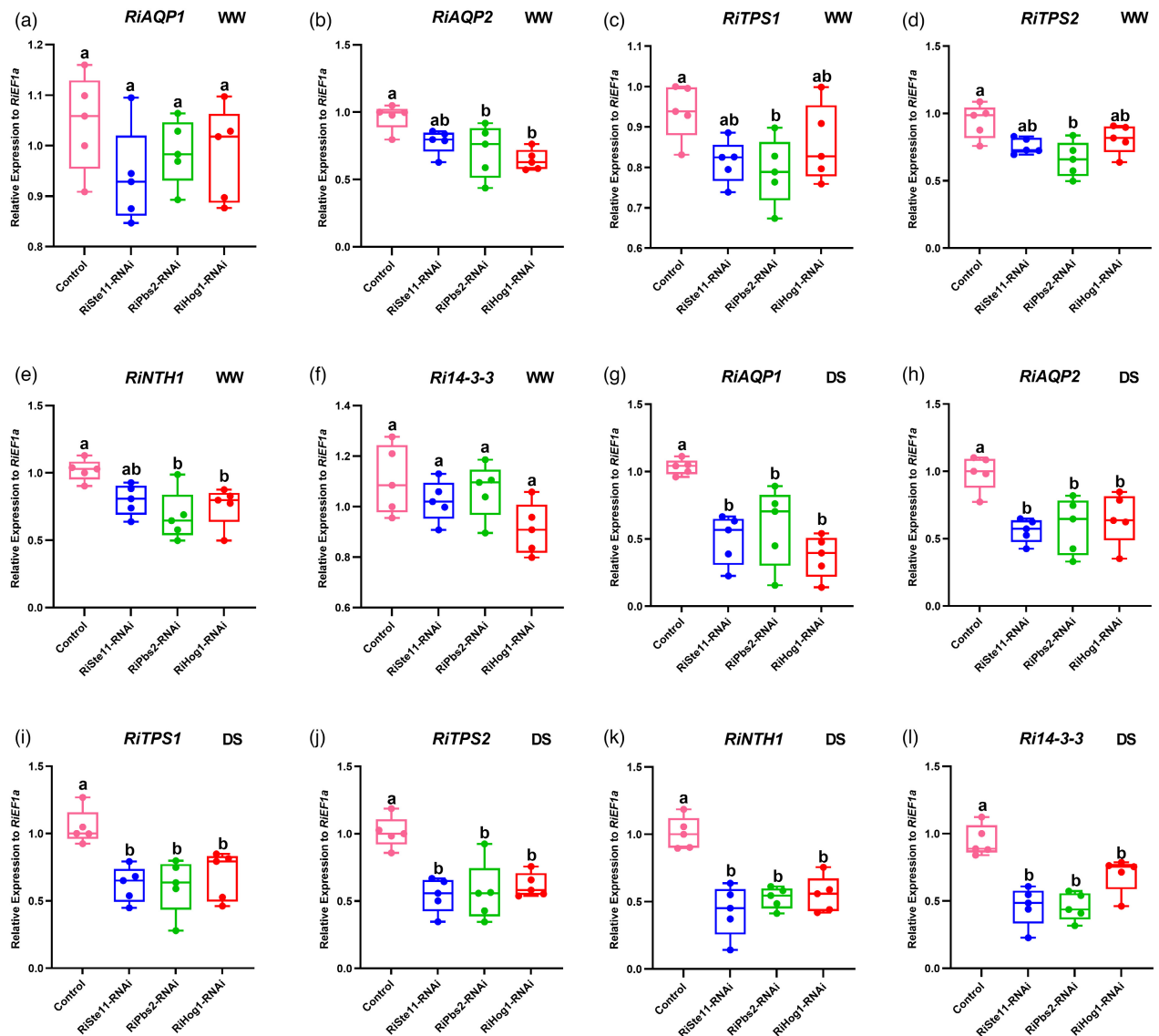


Figure 7 Knock-down of *RiSte11*, *RiPbs2* or *RiHog1* via host-induced gene silencing affects the expression levels of downstream genes *RiAQP1/2*, *RiTPS1/2*, *RiNTH1*, *Ri14-3-3*. The downstream genes of HOG1-MAPK cascade are identified to be *AQP* (encoding Aquaporin), *TPS* (encoding Trehalose-6-phosphate synthase), *NTH* (encoding Neutral trehalase) and *Ri14-3-3* (Sun et al., 2018). (a–f) Expression levels of *RiAQP1*, *RiAQP2*, *RiTPS1*, *RiTPS2*, *RiNTH1* and *Ri14-3-3* in control, *RiSte11-RNAi*, *RiPbs2-RNAi* or *RiHog1-RNAi* roots of *Astragalus sinicus* with *Rhizophagus irregularis* under well water condition. (g–l) Expression levels of *RiAQP1*, *RiAQP2*, *RiTPS1*, *RiTPS2*, *RiNTH1* and *Ri14-3-3* in control, *RiSte11-RNAi*, *RiPbs2-RNAi* or *RiHog1-RNAi* roots of *A. sinicus* with *R. irregularis* under drought stress. *R. irregularis RIEF1a* was used as the reference gene for normalization. Error bars represent the means of five biological replicates \pm SE. The different letters indicate significantly statistical differences between treatments at $P < 0.05$, based on one-way ANOVA, Tukey's test.

drought tolerance at the symbiotic interface of arbuscular mycorrhizas. Previous research showed DS up-regulated the levels of AM fungal MAPK transcripts in mycorrhizal plant roots (Liu et al., 2015b) and, thus, supported our results (Figure 2i–k). Therefore, we hypothesized that the AM fungal HOG1-MAPK cascade is necessary in response to plant-fungus AM symbiosis to drought.

Furthermore, EhHOG1 from fungus *Eurotium herbariorum* and PiHOG1 from *Piriformospora indica* can complement the growth defect of the yeast mutant Δ Hog1 strain under high osmotic stress conditions (Jin et al., 2005; Jogawat et al., 2016). Mutants of Ste11, Pbs2 and Hog1 also exhibited elevated sensitivity to osmotic stress in yeast (Alonso-Monge et al., 2001). Considering

our results, it can, thus, be said *RiSte11*, *RiPbs2* and *RiHog1* of *R. irregularis* play important roles in response to drought. ScHog1 in *S. cerevisiae* and PpHog1 in *Pichia pastoris* can translocate between the cytoplasm and nucleus in response to osmolarity environments, which is an important mechanism of activating or repressing their target genes (Reiser et al., 1999; Wang et al., 2021). Our findings imply the importance of nucleus-localized *RiHog1* protein in AM fungal symbiont in response to DS. Moreover, the pull-down result in our study was in accordance with the interaction of Ste11 with Pbs2, Pbs2 with Hog1 in yeast (Murakami et al., 2008; Tatebayashi et al., 2020). The importance of Pbs2 and Hog1 kinases in regulating stress tolerance has been demonstrated in different kinds of fungi

(Arana *et al.*, 2005; Day *et al.*, 2018; Jogawat *et al.*, 2016; Liu *et al.*, 2017). The results showed the potential role of RiHog1 in receiving drought signal from RiSte11 to RiPbs2 and transmitting the signal into the nucleus. According to previous studies, RiSte11 also could receive the signal from DS sensor sho1, then rely on it to the MAP Kinase Kinase Pbs2, which could transmit the signal to Hog1 in yeast cells (Hamel *et al.*, 2012; Zarrinpar *et al.*, 2004). In addition, whether the phosphorylation mechanism exists among these three HOG1-MAPK proteins needed to be further studied.

The importance of the HOG1-MAPK cascade in regulating plant root colonization/infection, and stress tolerance has been demonstrated in beneficial and pathogenic fungi (Jogawat *et al.*, 2016; Tian *et al.*, 2016). Nevertheless, the functions of *RiSte11*, *RiPbs2* and *RiHog1* during AM development are still unclear. In this study, the VIGS or HIGS of *RiSte11*, *RiPbs2* or *RiHog1* within roots colonized with *R. irregularis* showed collapsed arbuscules and hyphae with septa under DS (Figures 5 and 6), indicating the significance of *RiSte11*, *RiPbs2* and *RiHog1* for AM development. It is proposed the osmosis stress transmit by HOG1-MAPK cascade acts as a signal to the AM fungal symbiont developing within plant roots. This view is consistent with the previous research that AM fungal 14–3–3 protein is involved in arbuscule formation under abiotic stress (Sun *et al.*, 2018). The HOG1-MAPK cascade may affect the arbuscule development by regulating *Ri14-3-3* gene. Moreover, the expression levels of MAPK-related genes in *N. benthamiana* were not affected in the RNAi lines (Figure S11), coupled with that Xie *et al.* (2022) confirmed that the non-target gene (similar to the targeted gene) expression was not suppressed in the targeted RNAi lines. Therefore, it is reasonable to believe that silencing of *RiSte11*, *RiPbs2* and *RiHog1* did not affect the non-target genes of plants and other microorganisms. Knock-down of HOG1-MAPK cascade genes in *R. irregularis* also affected plants' physiological parameters, indicating that silencing of *RiSte11*, *RiPbs2* or *RiHog1* influenced the coordinating regulation of *R. irregularis*-plants symbiosis in response to DS.

It has been demonstrated that AQPs, trehalose-6-phosphate synthase (TPS) and neutral trehalase (NTH) genes are important factors in response to osmotic stress in plant-microorganism interactions (Iturriaga *et al.*, 2009; Li *et al.*, 2013, 2017; Ocón *et al.*, 2007). For example, TPS and neutral trehalase (NTH1) genes could improve plant resistance to osmotic stress (Acosta-Pérez *et al.*, 2020; Liu *et al.*, 2015a; Ocón *et al.*, 2007). Li *et al.* (2013) cloned two functional AQP genes from *G. intraradices* and proposed MAPK cascade may initiate gene expression to cope with osmotic stress. Our study confirmed that *RiSte11*, *RiPbs2* and *RiHog1* genes could regulate the expressions of drought-resistant genes in *R. irregularis* in response to DS (Figure 7), suggesting AM fungal HOG1-MAPK cascade genes improve plants' drought tolerance by regulating drought-resistant genes. Although the expression levels of *RiAQP2*, *RiTPS1/2* and *RiNTH1* were also decreased in some *RiSte11*-RNAi or *RiPbs2*-RNAi lines compared with the control under WW condition, it can be explained that the regulation of HOG1-MAPK cascade and downstream drought-resistant gene may incompletely depend on DS. However, further research about this phenomenon is required.

Based on our findings, we propose a working model in which *R. irregularis* HOG1-MAPK cascade regulates the drought-resistant genes in response to DS (Figure 8) to maintain A< development. Under DS, *A. sinicus* and AM fungus *R. irregularis*

can establish symbiosis. Higher expression levels of *RiSte11* (MAPKKK), *RiPbs2* (MAPKK) and *RiHog1* (MAPK) were detected during AM symbiosis under DS, indicating *RiSte11* may be activated by stimulated receptor (or related kinase) and then relays signal to *RiPbs2*, leading to the activation of *RiHog1* through direct protein-protein interaction (Hamel *et al.*, 2012). As a result, MAP kinase *RiHog1* enters the nucleus and further transmits the signal to the putative transcription factor (TF) to activate the expression of downstream drought-resistant genes (such as *RiAQP1*, *RiAQP2*, *RiTPS1*, *RiTPS2*, *RiNTH1* and *Ri14-3-3*). The knock-down of *RiSte11*, *RiPbs2* and *RiHog1* leads to decreased expressions of drought-resistant-related genes and collapse arbuscules, suggesting that *R. irregularis* HOG1-MAPK cascade proteins are essential for arbuscule development under DS. In future studies, functions of the potential sensor *RiSho1* and its putative interactions *RiCDC42/RiSte20* in response to DS should be characterized (Hamel *et al.*, 2012). It is important to confirm how the three HOG1-MAPK proteins transmit stress signals, and whether the *RiHog1* directly interacts with the potential TF (such as *Msn2*) to control downstream drought-resistant-related genes (Sun *et al.*, 2018).

In conclusion, we identified three HOG1-MAPK cascade genes, *RiSte11*, *RiPbs2* and *RiHog1* from AM fungus *R. irregularis*. The three HOG1-MAPK cascade genes showed high expression levels during mycorrhizal symbiosis and they were induced by DS. Based on the VIGS and HIGS results, it was affirmed that AM fungal HOG1-MAPK cascade genes were essential for arbuscule development and contributed to plant tolerance to DS. Importantly, the knock-down of HOG1-MAPK genes resulted in the decreased expression of drought-resistant genes in AM fungus. Our results provide physiological and molecular evidence for AM fungus improving plant drought tolerance as well as insights into AM fungal HOG1-MAPK cascade regulating arbuscule development under DS.

Experimental procedures

Biological materials and growth conditions

The AM fungus used in this study is *R. irregularis* DAOM197198, which was kindly provided by Dr. Jianyong An (Huazhong Agricultural University, Wuhan, China). Spores of *R. irregularis* are propagated on *Trifolium repens* L.

Astragalus sinicus L. was used in the gene expression analysis and the HIGS experiment. For the time-course experiment, the plant roots colonized with *R. irregularis* were harvested at 14-, 21-, 28-, 35-, 42-, 49- and 56-dpi (days post inoculation). Tobacco (*N. benthamiana*) was used in this study for the VIGS experiment. The seedlings of *A. sinicus* or *N. benthamiana* were inoculated with ~500 germinating spores/seedlings. The pot cultures contained a vermiculite and sand mix (v/v, 1:3). Plants were grown in controlled conditions, with a temperature of 24°C/18°C Day/night, 16/8-h light/dark cycle and relative humidity of 65%. All plants were watered twice per week with a modified Long-Ashton (mLA) nutrient solution containing 30 μM NaH₂PO₄ (Hewitt, 1966).

Yeast strains, wild-type BY4741 (Euroscarf acc. num. Y00000: MATα; *his3Δ1*; *leu2Δ0*; *met15Δ0*; *ura3Δ0*); *Δste11* (Euroscarf acc. num. Y05271: BY4741; MATα; *his3Δ1*; *leu2Δ0*; *met15Δ0*; *ura3Δ0*; YLR362w::kanMX4); *Δpbs2* (Euroscarf acc. num. Y07101: BY4741; MATα; *his3Δ1*; *leu2Δ0*; *met15Δ0*; *ura3Δ0*; YJL128c::kanMX4); *Δhog1* (Euroscarf acc. num. Y02724: BY4741: MATα; *his3Δ1*; *leu2Δ0*; *met15Δ0*; *ura3Δ0*; YLR113w::kanMX4).

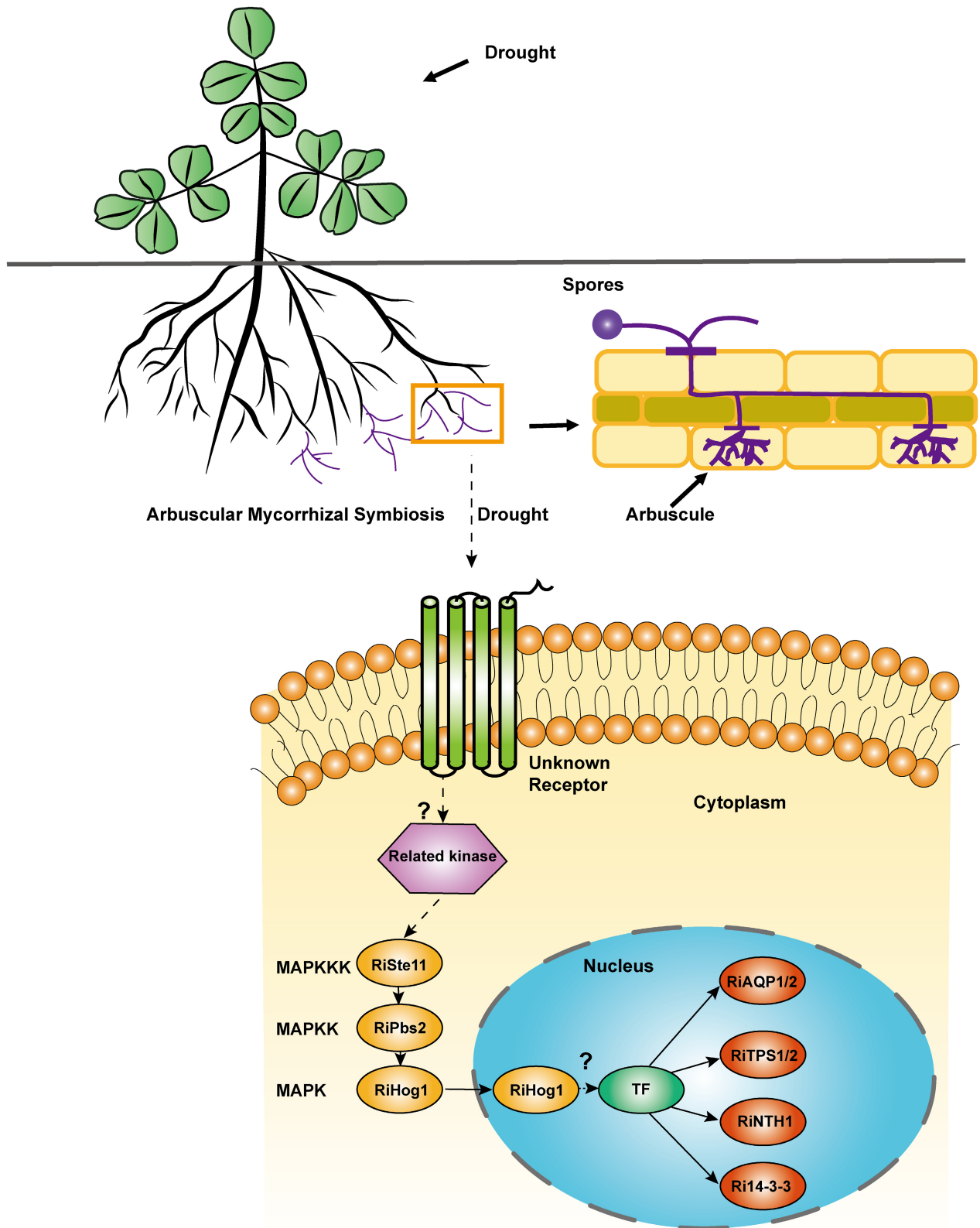


Figure 8 Proposed working model in which the *Rhizophagus irregularis* HOG1-MAPK cascade regulates arbuscule development and drought-resistant genes during AM symbiosis in response to drought stress. The picture shows that *Astragalus sinicus* is colonized with *R. irregularis* to establish a symbiosis relationship. In *R. irregularis*, the perception of the drought stress signal via the unidentified receptor, which may transmit the signal to the MAP kinase cascade through related kinases (homologues Cdc42 GTPase and Ste20 PAK-like kinase in yeasts) (Hamel *et al.*, 2012). Higher expression levels of *RiSte11* (MAPKKK), *RiPbs2* (MAPKK) and *RiHog1* (MAPK) were detected during AM symbiosis under drought stress, indicating *RiSte11* may be activated by stimulated receptor (or related kinase) and then relays the signal to *RiPbs2*, leading to the activation of *RiHog1* through direct protein–protein interaction. As a result, MAP kinase *RiHog1* enters the nucleus and further transmits the signal to the putative transcription factor (TF) to activate the expression of downstream drought-resistant genes (such as *RiAQP1*, *RiAQP2*, *RiTSP1*, *RiTSP2*, *RiNTH1* and *Ri14-3-3*).

Water treatment

In the pot system, the *A. sinicus* seedlings were colonized with *R. irregularis* and grown under normal water conditions for 28 days. Then plants were treated by 75% FWC, 50% FWC and 25% FWC for additional 14 days, respectively. In the HIGS and VIGS experiments, the plants were inoculated without (NM) or with *R. irregularis* (AM) for 28 days, then treated by WW (75% FWC) or DS (25%FWC) for additional 14 days. All plants were collected at 42 dpi and then stored at -80°C for subsequent analyses.

Genomic and transcriptomic data analyses of *Rhizophagus irregularis*

The *R. irregularis* HOG1-MAPK cascade gene sequences *RiSte11*, *RiPbs2* and *RiHog1* were obtained from the DDBJ and GEO databases (Morin *et al.*, 2019; Zeng *et al.*, 2018, 2020). DESeq2-normalized expression data of *RiSte11*, *RiPbs2*, *RiHog1*, *RiAQP1/2*, *RiTSP1/2*, *RiNTH1*, at six different developmental stages of *R. irregularis*, were plotted in heatmaps for comparison. Heatmaps were generated with the CLC Genomics Workbench (v20) software. Expression values (FPKM) calculation and expressed gene analysis (FDR-corrected $P < 0.05$, Benjamini–Hochberg test) were performed as described in Morin *et al.* (2019). The details are described in supporting methods S1.

Gene expression analysis

Total RNA was extracted from different tissues of *R. irregularis* and mycorrhizal roots using Fungal RNA Kit (OMEGA-R6840) according to the manufacturers' instructions, and the first-strand cDNA synthesis was initiated with the HiScript III reverse transcriptase (Vazyme-R323-01, Nanjing, China). Real-time qRT-PCR reactions were performed in a 96-well Real-time PCR system (Bio-Rad). All the reactions were performed with three technical replicates of three biological replicates. The *R. irregularis* *RiEF1a*, *A. sinicus* *AsActin*, *N. benthamiana* *NbtEF1a* were used as the endogenous reference gene for normalization, respectively. Relative expression levels of target genes were computed by the $2^{-\Delta\Delta\text{Ct}}$ method of relative quantification. A list of gene-specific primers used for real-time qRT-PCR is given in Table S2.

Heterologous expression in yeast

The open reading frames of *RiSte11*, *RiPbs2* or *RiHog1* were inserted into the yeast expression vector pFL61 (Minet *et al.*, 1992). The resulting plasmid *pFL61-RiSte11*, *pFL61-RiPbs2* or *pFL61-RiHog1* was transformed into yeast mutant Δste11 , Δpbs2 , Δhog1 strains via PEG/LiAc-mediated transformation, respectively (Gietz and Schiestl, 2007). The transformants adjusted to an OD_{600} of 0.2. Subsequently, serial dilutions ($\times 10$, $\times 100$, $\times 1000$ and $\times 10\,000$) were plated on SD/-URA

solid medium containing 0.0, 0.5, 1.0 or 1.5 M sorbitol, and 2% glucose was added as the carbon source. Growth was recorded after 3 days at 30°C .

For yeast growth analysis under osmotic stress, overnight cultures of different transformed cells in the SD/-URA liquid medium. The starting inoculation was adjusted to an OD_{600} of 0.12. The cells were incubated in SD/-URA liquid medium containing 1 M sorbitol at 30°C in a shaking incubator (200 rpm), during which samples were taken every 4 h. Each growth assay was replicated independently three times.

The subcellular localization in yeast was performed by fusing the N-terminus of *RiSte11*, *RiPbs2* or *RiHog1* to a green fluorescent protein (GFP). The ORFs of *RiSte11*, *RiPbs2* and *RiHog1* were inserted into the yeast expression vector pUG36 carrying the GFP reporter gene (Niedenthal *et al.*, 1996). The resulting plasmid *pUG36-RiSte11*, *pUG36-RiPbs2* or *pUG36-RiHog1* was transformed into EY57 cells as described above.

Virus-induced gene silencing

Tobacco rattle virus (TRV)-based expression vectors pTRV1 and pTRV2 were used in the experiment as described previously (Zhang and Liu, 2014). A 228 bp of *RiSte11* at 5' end or a 235 bp of *RiSte11* at 3' end, a 262 bp fragment of *RiPbs2* at 5' coding region or 287 bp of *RiPbs2* at 3' end, a 338 bp of the *RiHog1* cDNA at 5' end or a 241 bp fragment of *RiHog1* cDNA at 3' end was, respectively, PCR-amplified using primers (Table S2), the specific regions are shown in Figure S13. The three amplified target fragments were inserted into the pTRV2. The resulting plasmids, *pTRV2-RiSte11*, *pTRV2-RiPbs2*, *pTRV2-RiHog1* and pTRV1 were transformed into *Agrobacterium tumefaciens* GV3101, respectively. The 6-leaf-stage *N. benthamiana* plants were selected to infiltrate the re-suspended *Agrobacterium* culture into leaves. After 2 weeks of inoculation, plant roots and leaves were harvested to conduct subsequent experiments.

Host-induced gene silencing

The gateway vectors (Invitrogen) were used for the HIGS experiment. Constructs were created as described by Sun *et al.* (2018). The specific region of *RiSte11*, *RiPbs2* and *RiHog1* are designed as the VIGS experiment. The amplified fragments were recombined into the entry vector pDONR221 (Invitrogen), then the LR reaction was recombined the target sequence into the destination vector pK7GWIWG2D(II)-RootRed (Limpens *et al.*, 2004) according to the instructions in Gateway protocol. The corresponding Cheap-RNAi empty vector was used as the control. The *Agrobacterium rhizogenes* K599 carrying the resulting plasmids was used for the generation of *A. sinicus* hairy roots. Red fluorescence from the DsRed reporter was detected in the transgenic hairy roots using a fluorescence stereomicroscope

(Nikon, SMZ18). The hairy roots with strong red fluorescence were selected for subsequent experiments.

In vitro pull-down experiment

For the pull-down assay, the full-length CDS of *RiSte11* was fused to pETMALC-H, *RiPbs2* was fused to pET-32a and pGEX, *RiHog1* was fused to pGEX to generate MBP-*RiSte11*, His-*RiPbs2*, GST-*RiPbs2* and GST-*RiHog1* constructs. Recombinant proteins were separately expressed in *Escherichia coli* DE3 cells (Transgen, China) by growing cultures to $OD_{600} = 0.6$ at 20°C. And recombinant proteins were induced with 0.2 mM IPTG for 12 h. Purified MBP-*RiSte11*, MBP (negative control) proteins were incubated with MBP amylose beads (New England Biolabs, E8035) and GST-*RiHog1*, GST (negative control) proteins were incubated with GST amylose agarose beads (Thermo Scientific, 78 601) at 4°C for 1 h. After washing the beads five times with PBS buffer, GST-*RiPbs2* with MBP-*RiSte11* or MBP, His-*RiPbs2* with GST-*RiHog1* or GST were pulled down at 4°C for 2 h. Then the bound proteins were boiled in 5× SDS sample buffer. Samples were subjected to the subsequent separation on an SDS-PAGE gel and immunoblotting analysis using anti-MBP (Abmart, M20051), anti-His (Abmart, M20001) and anti-GST (Abmart, M20007) antibodies as described in Situ et al. (2020).

Quantification of mycorrhizal colonization

AM roots were digested in 10% KOH (w/v) at 90°C for 30 min, washed in 2% HCl (v/v) for 10 min and then washed three times with sterile water. Roots were stained with 5.0 µg/mL wheat germ agglutinin (WGA) Alexa Fluor 488 conjugates (Invitrogen) for 30 min at 37°C and washed in 1 × HBSS (Hanks' Balanced Salt Solution). Mycorrhizal colonization was quantified according to the MYCOCALC program (<http://www2.dijon.inra.fr/mychintec/Mycocalc-prg/download.html>) as described previously (Trouvelot et al., 1986).

Microscopy

A NiKon Eclipse Ni-U fluorescence microscope was used to examine the mycorrhizal colonization of plant roots. The *A. sinicus* transgenic roots with DsRed fluorescence were selected using a NiKon SMZ18 fluorescence stereomicroscope. Zeiss 780 laser scanning confocal microscope was used to observe the subcellular localization of GFP-fusion constructs in *S. cerevisiae* and arbuscule phenotype in the VIGS and HIGS experiments. GFP signal was detected using an excitation wavelength of 488 nm and emission between 500 and 550 nm, while DAPI signal was detected using an excitation wavelength of 345 nm and emission at 455 nm.

Trehalose content analysis

A Trehalose Extraction Kit (Solarbio, BC0330, Beijing, China) was used to examine the trehalose content. Transformed yeast cells were cultured in 100 mL SD/-URA medium without or with 1 M sorbitol. The starting inoculation was adjusted to an OD_{600} of 0.1. And cultured samples were taken at 24 h after sorbitol treatment. Then the trehalose content was measured at 620 nm with a UV/vis spectrophotometer (Mapada, Shanghai, China). Each growth assay was replicated independently three times.

Proline content analysis

The extraction and determination of proline in plants were performed according to Bates et al. (1973). Briefly, plant leaves

were frozen with liquid N₂ and grounded into powder. Then the proline content was measured at 520 nm with a UV/vis spectrophotometer (Mapada, Shanghai, China). Proline content was calculated on the basis of a proline standard curve. Data were expressed as µg g⁻¹ FW.

Field water capacity and relative water content measurements

The FWC was measured as described previously (Janeczko et al., 2016). The sand in the pot was placed into a pallet with water for 24 h. Then the pot was left to allow the excess water to drip off. The mass of sand in the pot was defined as M1. Subsequently, the sand was dried and weighed to yield M2. The maximum (100%) field soil water capacity was calculated from the M1-M2 subtraction. The obtained data allowed us to estimate the amount of water that is necessary to hydrate the soil at 75%, 50% and 25% of the maximum water capacity.

To determine the RWC in plants, fresh plants leaves were weighed immediately to get the FW, these leaves were then soaked in deionized water for 4 h and saturated weight (SW) was determined, these leaves were dried for 48 h at 75°C to determine the dry weight (DW). RWC in leaves was calculated as: $RWC = (FW - DW)/(SW - DW) \times 100\%$.

Bioinformatics

Molecular weight and isoelectric point (IP) are predicted by the ProtParam (<http://www.expasy.org/tools/protparam>). Homology modelling of the AM fungal MAPK cascade proteins was predicted by the program Swiss Model (<http://swissmodel.expasy.org/>). The ORFs of AM fungal MAPK genes are predicted by the ORF Finder (<https://www.ncbi.nlm.nih.gov/orffinder/>). The domains are indicated through the SMART program (<http://smart.embl-heidelberg.de/>).

Phylogenetic analysis

Analysis of the gene sequences was carried out using the NCBI Blast Server for the homology searches (www.ncbi.nlm.nih.gov). MEGA7 software (Kumar et al., 2016) was used to perform phylogenetic analysis. The multiple sequence alignment was progressed by ClustalW, and then the aligned sequences were loaded into MEGA7 for phylogenetic analysis. A phylogenetic tree was constructed using 1000 bootstrap replicates. The evolutionary history was inferred using the Neighbour-Joining method. Accession numbers of the predicted proteins are given in Table S3.

Statistical analyses

The one-way ANOVA with Tukey's test was used to make multiple comparisons. Averages with different letters indicate a significant difference at $P < 0.05$. Differences are described as statistical significance marked with asterisks for values of * $P < 0.05$ and ** $P < 0.01$.

Accession numbers

Sequence data from this article can be found in the AM fungal Genome databases and GenBank libraries under the following accession numbers for HOG1-MAPK proteins: *R. irregularis* *RiSte11* (XP_025172837.1), *RiPbs2* (XP_025178881.1), *RiHog1* (XP_025185210.1), *G. rosea* *GigrHog1* (RIB04295.1), *R. clarus* *RcHog1* (GET01709.1), *G. margarita* *GigmHog1* (KAF0432463.1), *G. cerebriforme* *GcHog1* (RIA92778.1), *R. diaphanous* *RdHog1*

(RGB42528.1), *S. cerevisiae* ScHog1 (NP_013214.1). Other accession numbers of the predicted proteins are given in Table S3.

Acknowledgements

The authors are grateful to Dr. An Jianyong (Huazhong Agricultural University, Wuhan, China) for kindly providing spores of *R. irregularis* and gateway vectors for this study. We would like to thank Dr. Luisa Lanfranco and Dr. Veronica Volpe (University of Turin, Italy) for kindly providing the pFL61 vector and EY57 strains for the yeast expression, respectively.

Funding

This work was supported by grants from the National Natural Science Foundation of China (grant no. 32071639, 32170116), the Laboratory of Lingnan Modern Agriculture Project (grant no. NZZ021025), Key Projects of Guangzhou of Science and Technology Plan (grant no. 201904020022).

Conflicts of interest

The authors declare no conflicts of interest.

Author contributions

H.C., M.T. and X.X. designed the study and experiments. S.W. performed experiments. S.W., X.X. and X.C. performed data analysis. S.W., Y.R. and W.L. performed the experiment of plant management. X.F. and H.W. assisted with the interpretation of the results. S.W., X.X., H.C. and M.T. wrote the article. M.T. and H.C. acquired the funding, administrated the project and supervised it.

References

- Acosta-Pérez, P., Camacho-Zamora, B.D., Espinoza-Sánchez, E.A., Gutiérrez-Soto, G., Zavala-García, F., Abraham-Juárez, M.J. and Sinagawa-García, S.R. (2020) Characterization of trehalose-6-phosphate synthase and trehalose-6-phosphate phosphatase genes and analysis of its differential expression in Maize (*Zea mays*) seedlings under drought stress. *Plan. Theory* **9**, 315.
- Alonso-Monge, R.E., Wojda, I., Bebelman, J.P., Mager, W.H. and Siderius, M. (2001) Hyperosmotic stress response and regulation of cell wall integrity in *Saccharomyces cerevisiae* share common functional aspects. *Mol. Microbiol.* **41**, 717–730.
- An, J., Zeng, T., Ji, C., de Graaf, S., Zheng, Z., Xiao, T.T., Deng, X. *et al.* (2019) A *Medicago truncatula* SWEET transporter implicated in arbuscule maintenance during arbuscular mycorrhizal symbiosis. *New Phytol.* **224**, 396–408.
- Arana, D.M., Nombela, C., Alonso-Monge, R. and Pla, J. (2005) The Pbs2 MAP kinase kinase is essential for the oxidative-stress response in the fungal pathogen *Candida albicans*. *Microbiology* **151**, 1033–1049.
- Augé, R.M. (2001) Water relations, drought and vesicular-arbuscular mycorrhizal symbiosis. *Mycorrhiza* **11**, 3–42.
- Bago, B., Pfeffer, P.E., Abubaker, J., Jun, J., Allen, J.W., Brouillette, J., Douds, D.D. *et al.* (2003) Carbon export from arbuscular mycorrhizal roots involves the translocation of carbohydrate as well as lipid. *Plant Physiol.* **131**, 1496–1507.
- Bates, L.S., Waldren, R.P. and Teare, I.D. (1973) Rapid determination of free proline for water-stress studies. *Plant Soil* **39**, 205–207.
- Begum, N., Qin, C., Ahanger, M.A., Raza, S., Khan, M.I., Ashraf, M., Ahmed, N. *et al.* (2019) Role of arbuscular mycorrhizal fungi in plant growth regulation: implications in abiotic stress tolerance. *Front. Plant Sci.* **10**, 1068.
- Begum, N., Akhtar, K., Ahanger, M.A., Iqbal, M., Wang, P., Mustafa, N.S. and Zhang, L. (2021) Arbuscular mycorrhizal fungi improve growth, essential oil, secondary metabolism, and yield of tobacco (*Nicotiana tabacum* L.) under drought stress conditions. *Environ. Sci. Pollut. Res.* **28**, 45276–45295.
- Bonfante, P. and Genre, A. (2010) Mechanisms underlying beneficial plant–fungus interactions in mycorrhizal symbiosis. *Nat. Commun.* **1**, 48.
- Brundrett, M.C. and Tedersoo, L. (2018) Evolutionary history of mycorrhizal symbioses and global host plant diversity. *New Phytol.* **220**, 1108–1115.
- Chantreau, M., Chabbert, B., Billiard, S., Hawkins, S. and Neutelings, G. (2015) Functional analyses of cellulose synthase genes in flax (*Linum usitatissimum*) by virus-induced gene silencing. *Plant Biotechnol. J.* **13**, 1312–1324.
- Chen, E.C.H., Morin, E., Beaudet, D., Noel, J., Yildirim, G., Ndikumana, S., Charron, P. *et al.* (2018) High intraspecific genome diversity in the model arbuscular mycorrhizal symbiont *Rhizophagus irregularis*. *New Phytol.* **220**, 1161–1171.
- Chen, X., Ding, Y., Yang, Y., Song, C., Wang, B., Yang, S., Guo, Y. *et al.* (2021) Protein kinases in plant responses to drought, salt, and cold stress. *J. Integr. Plant Biol.* **63**, 53–78.
- Cheng, W., Song, X., Li, H., Cao, L., Sun, K., Qiu, X., Xu, Y. *et al.* (2015) Host-induced gene silencing of an essential chitin synthase gene confers durable resistance to *Fusarium* head blight and seedling blight in wheat. *Plant Biotechnol. J.* **13**, 1335–1345.
- Chitarra, W., Pagliarani, C., Maserti, B., Lumini, E., Siciliano, I., Cascone, P., Schubert, A. *et al.* (2016) Insights on the impact of arbuscular mycorrhizal symbiosis on tomato tolerance to water stress. *Plant Physiol.* **171**, 1009–1023.
- Colcombet, J. and Hirt, H. (2008) *Arabidopsis* MAPKs: a complex signalling network involved in multiple biological processes. *Biochem. J.* **413**, 217–226.
- Day, A.M., McNiff, M.M., Dantas, A.D.S., Gow, N.A.R., Quinn, J. and Mitchell, A.P. (2018) Hog1 regulates stress tolerance and virulence in the emerging fungal pathogen *Candida auris*. *mSphere* **3**, e506–e518.
- Deng, X., Elomaa, P., Nguyen, C.X., Hytönen, T., Valkonen, J.P.T. and Teeri, T.H. (2012) Virus-induced gene silencing for Asteraceae—a reverse genetics approach for functional genomics in *Gerbera hybrida*. *Plant Biotechnol. J.* **10**, 970–978.
- Ezawa, T., Maruyama, H., Kikuchi, Y., Yokoyama, K. and Masuta, C. (2020) Application of virus-induced gene silencing to arbuscular mycorrhizal fungi. *Methods Mol. Biol.* **2146**, 249–254.
- Genre, A., Lanfranco, L., Perotto, S. and Bonfante, P. (2020) Unique and common traits in mycorrhizal symbioses. *Nat. Rev. Microbiol.* **18**, 649–660.
- Ghag, S.B., Shekhawat, U.K.S. and Ganapathi, T.R. (2014) Host-induced post-transcriptional hairpin RNA-mediated gene silencing of vital fungal genes confers efficient resistance against *Fusarium* wilt in banana. *Plant Biotechnol. J.* **12**, 541–553.
- Gholamhoseini, M., Ghalavand, A., Dolatabadian, A., Jamshidi, E. and Khodaei-Joghan, A. (2013) Effects of arbuscular mycorrhizal inoculation on growth, yield, nutrient uptake and irrigation water productivity of sunflowers grown under drought stress. *Agric. Water Manag.* **117**, 106–114.
- Gianinazzi, S., Gollotte, A., Binet, M., van Tuinen, D., Redecker, D. and Wipf, D. (2010) Agroecology: the key role of arbuscular mycorrhizas in ecosystem services. *Mycorrhiza* **20**, 519–530.
- Gietz, R.D. and Schiestl, R.H. (2007) High-efficiency yeast transformation using the LiAc/SS carrier DNA/PEG method. *Nat. Protoc.* **2**, 31–34.
- Gutjahr, C. and Parniske, M. (2013) Cell and developmental biology of arbuscular mycorrhiza symbiosis. *Annu. Rev. Cell Dev. Biol.* **29**, 593–617.
- Hamel, L., Nicole, M., Duplessis, S. and Ellis, B.E. (2012) Mitogen-activated protein kinase signaling in plant-interacting fungi: distinct messages from conserved messengers. *Plant Cell* **24**, 1327–1351.
- Harrison, M.J. (2012) Cellular programs for arbuscular mycorrhizal symbiosis. *Curr. Opin. Plant Biol.* **15**, 691–698.
- Hartmann, M., Voß, S. and Requena, N. (2020) Host-Induced gene silencing of arbuscular mycorrhizal fungal genes via *Agrobacterium rhizogenes*-mediated root transformation in *Medicago truncatula*. *Methods Mol. Biol.* **2146**, 239–248.
- Hazzoumi, Z., Moustakime, Y., Hassan Elharchli, E. and Joutei, K.A. (2015) Effect of arbuscular mycorrhizal fungi (AMF) and water stress on growth, phenolic compounds, glandular hairs, and yield of essential oil in basil (*Ocimum gratissimum* L.). *Chem. Biol. Technol. Agric.* **2**, 10.

- Helber, N., Wippel, K., Sauer, N., Schaarschmidt, S., Hause, B. and Requena, N. (2011) A versatile monosaccharide transporter that operates in the arbuscular mycorrhizal fungus *Glomus* sp is crucial for the symbiotic relationship with plants. *Plant Cell* **23**, 3812–3823.
- Hewitt, E.J. (1966) *Sand and Water Culture Methods Used in the Study of Plant Nutrition*. England: Commonwealth Agricultural Bureaux.
- Hu, Y., Xie, W. and Chen, B. (2020) Arbuscular mycorrhiza improved drought tolerance of maize seedlings by altering photosystem II efficiency and the levels of key metabolites. *Chem. Biol. Technol. Agric.* **7**, 20.
- Huang, D., Ma, M., Wang, Q., Zhang, M., Jing, G., Li, C. and Ma, F. (2020) Arbuscular mycorrhizal fungi enhanced drought resistance in apple by regulating genes in the MAPK pathway. *Plant Physiol. Biochem.* **149**, 245–255.
- Iturriaga, G., Suárez, R. and Nova-Franco, B. (2009) Trehalose metabolism: from osmoprotection to signaling. *Int. J. Mol. Sci.* **10**, 3793–3810.
- Janeczko, A., Gruszka, D., Pocięcha, E., Dziurka, M., Filek, M., Jurczyk, B., Kalaji, H.M. et al. (2016) Physiological and biochemical characterisation of watered and drought-stressed barley mutants in the *HvDWARF* gene encoding C6-oxidase involved in brassinosteroid biosynthesis. *Plant Physiol. Biochem.* **99**, 126–141.
- Ji, Y., Yang, F., Ma, D., Zhang, J., Wan, Z., Liu, W. and Li, R. (2012) HOG-MAPK signaling regulates the adaptive responses of *Aspergillus fumigatus* to thermal stress and other related stress. *Mycopathologia* **174**, 273–282.
- Jiang, Y., Wang, W., Xie, Q., Liu, N., Liu, L., Wang, D., Zhang, X. et al. (2017) Plants transfer lipids to sustain colonization by mutualistic mycorrhizal and parasitic fungi. *Science* **356**, 1172–1175.
- Jiang, C., Zhang, X., Liu, H. and Xu, J. (2018) Mitogen-activated protein kinase signaling in plant pathogenic fungi. *PLoS Pathog.* **14**, e1006875.
- Jin, Y., Weining, S. and Nevo, E. (2005) A MAPK gene from Dead Sea fungus confers stress tolerance to lithium salt and freezing–thawing: Prospects for saline agriculture. *Proc Natl Acad Sci U S A.* **102**, 18992–18997.
- Jogawat, A., Vadassery, J., Verma, N., Oelmüller, R., Dua, M., Nevo, E. and Johri, A.K. (2016) PIHOG1, a stress regulator MAP kinase from the root endophyte fungus *Piriformospora indica*, confers salinity stress tolerance in rice plants. *Sci. Rep.* **6**, 36765.
- Kou, Y. and Naqvi, N.I. (2016) Surface sensing and signaling networks in plant pathogenic fungi. *Semin. Cell Dev. Biol.* **57**, 84–92.
- Kumar, S., Stecher, G. and Tamura, K. (2016) MEGA7: molecular evolutionary genetics analysis version 7.0 for bigger datasets. *Mol. Biol. Evol.* **33**, 1870–1874.
- Lenoir, I., Fontaine, J. and Lounès-Hadj, S.A. (2016) Arbuscular mycorrhizal fungal responses to abiotic stresses: a review. *Phytochemistry* **123**, 4–15.
- Leyva-Morales, R., Gavito, M.E. and Carrillo-Saucedo, S.M. (2019) Morphological and physiological responses of the external mycelium of *Rhizophagus intraradices* to water stress. *Mycorrhiza* **29**, 141–147.
- Li, L., Ye, Y., Pan, L., Zhu, Y., Zheng, S. and Lin, Y. (2009) The induction of trehalose and glycerol in *Saccharomyces cerevisiae* in response to various stresses. *Biochem. Biophys. Res. Commun.* **387**, 778–783.
- Li, T., Hu, Y., Hao, Z., Li, H., Wang, Y. and Chen, B. (2013) First cloning and characterization of two functional aquaporin genes from an arbuscular mycorrhizal fungus *Glomus intraradices*. *New Phytol.* **197**, 617–630.
- Li, T., Hou, W., Ruan, Y., Chen, B., Yang, L., Zhou, C. and Zhu, Y. (2017) Structural features of the aromatic/arginine constriction in the aquaglyceroporin *GintAQPF2* are responsible for glycerol impermeability in arbuscular mycorrhizal symbiosis. *Fungal Biol.* **121**, 95–102.
- Limpens, E., Ramos, J., Franken, C., Raz, V., Compaan, B., Franssen, H., Bisseling, T. et al. (2004) RNA interference in *Agrobacterium rhizogenes*-transformed roots of *Arabidopsis* and *Medicago truncatula*. *J. Exp. Bot.* **55**, 983–992.
- Lin, X., Kaul, S., Rounsley, S., Shea, T.P., Benito, M., Town, C.D., Fujii, C.Y. et al. (1999) Sequence and analysis of chromosome 2 of the plant *Arabidopsis thaliana*. *Nature* **402**, 761–768.
- Lin, L., Wu, J., Jiang, M. and Wang, Y. (2021) Plant mitogen-activated protein kinase cascades in environmental stresses. *Int. J. Mol. Sci.* **22**, 1543.
- Liu, Y., Han, L., Qin, L. and Zhao, D. (2015a) *Saccharomyces cerevisiae* gene TPS1 improves drought tolerance in *Zea mays* L. by increasing the expression of SDD1 and reducing stomatal density. *Plant Cell Tissue Organ Cult.* **120**, 779–789.
- Liu, Z., Li, Y., Ma, L., Wei, H., Zhang, J., He, X. and Tian, C. (2015b) Coordinated regulation of arbuscular mycorrhizal fungi and soybean MAPK pathway genes improved mycorrhizal soybean drought tolerance. *Mol. Plant-Microbe Interact.* **28**, 408–419.
- Liu, J., Wang, Z., Sun, H., Ying, S. and Feng, M. (2017) Characterization of the Hog1 MAPK pathway in the entomopathogenic fungus *Beauveria bassiana*. *Environ. Microbiol.* **19**, 1808–1821.
- Luginbuehl, L.H., Menard, G.N., Kurup, S., Van Erp, H., Radhakrishnan, G.V., Breakspear, A., Oldroyd, G.E.D. et al. (2017) Fatty acids in arbuscular mycorrhizal fungi are synthesized by the host plant. *Science* **356**, 1175–1178.
- Martínez-Soto, D. and Ruiz-Herrera, J. (2017) Functional analysis of the MAPK pathways in fungi. *Rev. Iberoam. Micol.* **34**, 192–202.
- Minet, M., Dufour, M.E. and Lacroute, F. (1992) Complementation of *Saccharomyces cerevisiae* auxotrophic mutants by *Arabidopsis thaliana* cDNAs. *Plant J.* **2**, 417–422.
- Morin, E., Miyauchi, S., San Clemente, H., Chen, E.C.H., Pelin, A., de la Providencia, I., Ndikumana, S. et al. (2019) Comparative genomics of *Rhizophagus irregularis*, *R. cerebriforme*, *R. diaphanus* and *Gigaspora rosea* highlights specific genetic features in Glomeromycotina. *New Phytol.* **222**, 1584–1598.
- Murakami, Y., Tatebayashi, K. and Saito, H. (2008) Two adjacent docking sites in the yeast Hog1 mitogen-activated protein (MAP) kinase differentially interact with the Pbs2 MAP kinase kinase and the Ptp2 protein tyrosine phosphatase. *Mol. Cell. Biol.* **28**, 2481–2494.
- Niedenthal, R.K., Riles, L., Johnston, M. and Hegemann, J.H. (1996) Green fluorescent protein as a marker for gene expression and subcellular localization in budding yeast. *Yeast* **12**, 773–786.
- Ocón, A., Hampp, R. and Requena, N. (2007) Trehalose turnover during abiotic stress in arbuscular mycorrhizal fungi. *New Phytol.* **174**, 879–891.
- Parniske, M. (2008) Arbuscular mycorrhiza: the mother of plant root endosymbioses. *Nat. Rev. Microbiol.* **6**, 763–775.
- Püschel, D., Bitterlich, M., Rydlová, J. and Jansa, J. (2021) Drought accentuates the role of mycorrhiza in phosphorus uptake. *Soil Biol. Biochem.* **157**, 108243.
- Quiroga, G., Erice, G., Ding, L., Chaumont, F., Aroca, R. and Ruiz-Lozano, J.M. (2019) The arbuscular mycorrhizal symbiosis regulates aquaporins activity and improves root cell water permeability in maize plants subjected to water stress. *Plant Cell Environ.* **42**, 2274–2290.
- Reiser, V., Ruis, H. and Ammerer, G. (1999) Kinase activity-dependent nuclear export opposes stress-induced nuclear accumulation and retention of Hog1 mitogen-activated protein kinase in the budding yeast *Saccharomyces cerevisiae*. *Mol. Biol. Cell* **10**, 1147–1161.
- Román, E., Correia, I., Prieto, D., Alonso, R. and Pla, J. (2020) The HOG MAPK pathway in *Candida albicans*: more than an osmosensing pathway. *Int. Microbiol.* **23**, 23–29.
- Shrestha, A., Cudjoe, D.K., Kamruzzaman, M., Siddique, S., Fiorani, F., León, J. and Naz, A.A. (2021) Abscisic acid-responsive element binding transcription factors contribute to proline synthesis and stress adaptation in *Arabidopsis*. *J. Plant Physiol.* **261**, 153414.
- Situ, J., Jiang, L., Fan, X., Yang, W., Li, W., Xi, P., Deng, Y. et al. (2020) An RXLR effector PIvAh142 from *Peronosphythora litchii* triggers plant cell death and contributes to virulence. *Mol. Plant Pathol.* **21**, 415–428.
- Sun, Z., Song, J., Xin, X.A., Xie, X. and Zhao, B. (2018) Arbuscular mycorrhizal fungal 14-3-3 proteins are involved in arbuscule formation and responses to abiotic stresses during AM symbiosis. *Front. Microbiol.* **9**, 91.
- Tatebayashi, K., Yamamoto, K., Tomida, T., Nishimura, A., Takayama, T., Oyama, M., Kozuka-Hata, H. et al. (2020) Osmostress enhances activating phosphorylation of Hog1 MAP kinase by mono-phosphorylated Pbs2 MAP2K. *EMBO J.* **39**, e103444.
- Tian, L., Wang, Y., Yu, J., Xiong, D., Zhao, H. and Tian, C. (2016) The mitogen-activated protein kinase kinase VdPbs2 of *Verticillium dahliae* regulates microsclerotia formation, stress response, and plant infection. *Front. Microbiol.* **7**, 1532.
- Tisserant, E., Malbreil, M., Kuo, A., Kohler, A., Symeonidi, A., Balestrini, R., Charron, P. et al. (2013) Genome of an arbuscular mycorrhizal fungus provides insight into the oldest plant symbiosis. *Proc. Natl. Acad. Sci.* **110**, 20117–20122.

- Trouvelot, A., Kough, J.L. and Gianinazzi-Pearson, V. (1986) Mesure du taux de mycorrhization VA d'un système racinaire. Recherche de méthode d'estimation ayant une signification fonctionnelle. In *Physiological and Genetical Aspects of Mycorrhizae* (Gianinazzi-Pearson, V. and Gianinazzi, S., eds), pp. 217–221. Paris, France: INRA.
- Wang, B., Qin, X., Wu, J., Deng, H., Li, Y., Yang, H., Chen, Z. *et al.* (2016) Analysis of crystal structure of *Arabidopsis* MPK6 and generation of its mutants with higher activity. *Sci. Rep.* **6**, 25646.
- Wang, W., Shi, J., Xie, Q., Jiang, Y., Yu, N. and Wang, E. (2017) Nutrient exchange and regulation in arbuscular mycorrhizal symbiosis. *Mol. Plant* **10**, 1147–1158.
- Wang, M., Wilde, J., Baldwin, I.T. and Groten, K. (2018) *Nicotiana attenuata*'s capacity to interact with arbuscular mycorrhiza alters its competitive ability and elicits major changes in the leaf transcriptome. *J. Integr. Plant Biol.* **60**, 242–261.
- Wang, R., Zhao, T., Zhuo, J., Zhan, C., Zhang, F., Linhardt, R.J., Bai, Z. *et al.* (2021) MAPK/HOG signaling pathway induced stress-responsive damage repair is a mechanism for *Pichia pastoris* to survive from hyperosmotic stress. *J. Chem. Technol. Biotechnol.* **96**, 412–422.
- Xie, X., Huang, W., Liu, F., Tang, N., Liu, Y., Lin, H. and Zhao, B. (2013) Functional analysis of the novel mycorrhiza-specific phosphate transporter *AsPT1* and *PHT1* family from *Astragalus sinicus* during the arbuscular mycorrhizal symbiosis. *New Phytol.* **198**, 836–852.
- Xie, X., Lin, H., Peng, X., Xu, C., Sun, Z., Jiang, K., Huang, A. *et al.* (2016) Arbuscular mycorrhizal symbiosis requires a phosphate transporter in the *Gigaspora margarita* fungal symbiont. *Mol. Plant* **9**, 1583–1608.
- Xie, X., Lai, W., Che, X., Wang, S., Ren, Y., Hu, W., Chen, H. *et al.* (2022) A SPX domain-containing phosphate transporter from *Rhizophagus irregularis* handles phosphate homeostasis at symbiotic interface of arbuscular mycorrhizas. *New Phytol.* **234**, 650–671.
- Xu, J., Wang, X., Li, Y., Zeng, J., Wang, G., Deng, C. and Guo, W. (2018) Host-induced gene silencing of a regulator of G protein signalling gene (*VdRGS1*) confers resistance to *Verticillium* wilt in cotton. *Plant Biotechnol. J.* **16**, 1629–1643.
- Zarrinpar, A., Bhattacharyya, R.P., Nittler, M.P. and Lim, W.A. (2004) Sho1 and Pbs2 act as scaffolds linking components in the yeast high osmolarity MAP kinase pathway. *Mol. Cell* **14**, 825–832.
- Zeng, T., Holmer, R., Hontelez, J., Te Lintel-Hekkert, B., Marufu, L., de Zeeuw, T., Wu, F. *et al.* (2018) Host- and stage-dependent secretome of the arbuscular mycorrhizal fungus *Rhizophagus irregularis*. *Plant J.* **94**, 411–425.
- Zeng, T., Rodriguez-Moreno, L., Mansurkhodzaev, A., Wang, P., van den Berg, W., Gascioli, V., Cottaz, S. *et al.* (2020) A lysin motif effector subverts chitin-triggered immunity to facilitate arbuscular mycorrhizal symbiosis. *New Phytol.* **225**, 448–460.
- Zhang, H.L. and Liu, Y. (2014) VIGS assays. *Bio-protocol* **4**, e1057.
- Zhang, F., Zou, Y., Wu, Q. and Kuča, K. (2020) Arbuscular mycorrhizas modulate root polyamine metabolism to enhance drought tolerance of trifoliolate orange. *Environ. Exp. Bot.* **171**, 103926.
- Zhou, X., Ye, J., Zheng, L., Jiang, P. and Lu, L. (2019) A new identified suppressor of Cdc7p/SepH kinase, PomA, regulates fungal asexual reproduction via affecting phosphorylation of MAPK-HogA. *PLoS Genet.* **15**, e1008206.
- Zhu, J. (2016) Abiotic stress signaling and responses in plants. *Cell* **167**, 313–324.
- Zhu, D., Chang, Y., Pei, T., Zhang, X., Liu, L., Li, Y., Zhuang, J. *et al.* (2020) MAPK-like protein 1 positively regulates maize seedling drought sensitivity by suppressing ABA biosynthesis. *Plant J.* **102**, 747–760.
- Zhu, X., Zhang, N., Liu, X., Li, S., Yang, J., Hong, X., Wang, F. *et al.* (2021) Mitogen-activated protein kinase 11 (MAPK11) maintains growth and photosynthesis of potato plant under drought condition. *Plant Cell Rep.* **40**, 491–506.

Supporting information

Additional supporting information may be found online in the Supporting Information section at the end of the article.

Appendix S1

Figure S1 Effects of arbuscular mycorrhiza and non-mycorrhiza on the growth, relative water and proline contents of *Astragalus sinicus* in response to well water and drought stress.

Figure S2 Characteristics of *RiSte11*, *RiPbs2* and *RiHog1* in *Rhizophagus irregularis*.

Figure S3 Heatmap analysis of HOG1-MAPK cascade (*RiSte11*, *RiPbs2*, *RiHog1*) and drought-resistant genes (*RiAQP1/2*, *RiTSP1/2*, *RiNTH1*) in *Rhizophagus irregularis* under different developmental conditions.

Figure S4 Expressions of *RiSte11*, *RiPbs2* and *RiHog1* in *Rhizophagus irregularis* colonized roots of *Astragalus sinicus* at 42 days post inoculation (dpi) in response to drought stress.

Figure S5 Microscopy images of the composite *Astragalus sinicus* hairy roots with control, *RiSte11*, *RiPbs2* or *RiHog1* gene mediated by host-induced gene silencing.

Figure S6 Overall growth performance of the composite *Astragalus sinicus* with hairy roots carrying the empty vector (control), *RiSte11*-, *RiPbs2*- or *RiHog1*-RNAi construct mediated by host-induced gene silencing.

Figure S7 Host-induced gene silencing of HOG1-MAPK cascade genes in *Rhizophagus irregularis* affects the RWC and proline content in *Astragalus sinicus* leaves.

Figure S8 Virus-induced gene silencing of HOG1-MAPK cascade genes in *Rhizophagus irregularis* affects the RWC and proline content in *Nicotiana benthamiana* leaves.

Figure S9 Host-induced gene silencing of HOG1-MAPK cascade genes in *Rhizophagus irregularis* inhibits arbuscule development in roots under well water condition.

Figure S10 Molecular and arbuscular mycorrhizal phenotypes of virus-induced gene silencing of *RiSte11*, *RiPbs2* or *RiHog1* in *Nicotiana benthamiana* under well water condition.

Figure S11 Virus-induced gene silencing of *RiSte11*, *RiPbs2* or *RiHog1* in *Rhizophagus irregularis* does not affect expression levels of MAPK cascade genes in *Nicotiana benthamiana*.

Figure S12 The expression of *RiAQP1/2*, *RiTSP1/2*, *RiNTH1* and *Ri14-3-3* in response to drought stress.

Table S1 Characteristics of HOG1-MAPK cascade and drought-resistant genes in *Rhizophagus irregularis*.

Table S2 PCR primers used for HOG1-MAPK cascade genes in *Rhizophagus irregularis*.

Table S3 The accession numbers of fungal MAPK proteins used in this study.